

**PREPARATION OF NANOFILTRATION HOLLOW  
FIBER MEMBRANE FOR ACETIC ACID  
REMOVAL FROM SYNTHETIC HYDROLYSATE**

**NURLIN FATIN BT MOHD TAHIRUN**

**BACHELOR OF CHEMICAL ENGINEERING  
UNIVERSITI MALAYSIA PAHANG**

©NURLIN FATIN (2014)

## Thesis Access Form

No \_\_\_\_\_ Location \_\_\_\_\_

Author : Nurlin Fatin Bt Mohd Tahirun

Title : Preparation Of Nanofiltration Hollow Fiber Membrane For Acetic Acid Removal From Synthetic Hydrolysate

Status of access OPEN / ~~RESTRICTED~~ / ~~CONFIDENTIAL~~

Moratorium period: \_\_\_\_\_ years, ending \_\_\_\_\_ / \_\_\_\_\_ 200\_\_\_\_\_

Conditions of access proved by (CAPITALS): DR JOLIUS GIMBUN

Supervisor (Signature).....

Faculty: .....

Author's Declaration: *I agree the following conditions:*

OPEN access work shall be made available (in the University and externally) and reproduced as necessary at the discretion of the University Librarian or Head of Department. It may also be copied by the British Library in microfilm or other form for supply to requesting libraries or individuals, subject to an indication of intended use for non-publishing purposes in the following form, placed on the copy and on any covering document or label.

*The statement itself shall apply to ALL copies:*

**This copy has been supplied on the understanding that it is copyright material and that no quotation from the thesis may be published without proper acknowledgement.**

**Restricted/confidential work:** All access and any photocopying shall be strictly subject to written permission from the University Head of Department and any external sponsor, if any.

Author's signature.....Date: .....

users declaration: for signature during any Moratorium period (Not Open work):

***I undertake to uphold the above conditions:***

Date	Name (CAPITALS)	Signature	Address

**PREPARATION OF NANOFILTRATION HOLLOW  
FIBER MEMBRANE FOR ACETIC ACID  
REMOVAL FROM SYNTHETIC HYDROLYSATE**

NURLIN FATIN BT MOHD TAHIRUN

Thesis submitted in partial fulfilment of the requirements  
for the award of the degree of  
Bachelor of Chemical Engineering

**Faculty of Chemical & Natural Resources Engineering  
UNIVERSITI MALAYSIA PAHANG**

JULY 2014

©NURLIN FATIN (2014)

## **SUPERVISOR'S DECLARATION**

We hereby declare that we have checked this thesis and in my opinion, this thesis is adequate in terms of scope and quality for the award of the degree of Bachelor of Chemical Engineering.

Signature :  
Name of main supervisor : DR. SYED MOHD SAUFI BIN TUAN CHIK  
Position : SENIOR LECTURE  
Date : 30 JUNE 2014

## **STUDENT'S DECLARATION**

I hereby declare that the work in this thesis is my own except for quotations and summaries which have been duly acknowledged. The thesis has not been accepted for any degree and is not concurrently submitted for award of other degree.

Signature :  
Name : NURLIN FATIN BT MOHD TAHIRUN  
ID Number : KA10106  
Date : JULY 2014

*Dedication*

*To my parents and siblings*

## **ACKNOWLEDGEMENT**

Alhamdulillah, praised to God for giving us an opportunity to complete this course after struggling with all the problems and challenges in completing project for the past several months.

First and foremost I would like to extend our sincerest gratitude to Dr. Syed Mohd Saufi Bin Tuan Chik, my project supervisor for his willingness in overseeing the progress of my project assignments from its initial phases until the completion. I do believe that all his advice and comments are beneficial to produce the best result.

To my friends and course mates especially Siti Normunira, thank you for helping me through my stormy weathers. The experiences and knowledge I gained throughout the process of completing this project would enhance my knowledge and become well-equipped to face the challenges which lie in the future.

Lastly but not least, appreciation is extended to my family members, I can never enough for your love, and for supporting me throughout my studies in Universiti Malaysia Pahang (UMP).

## **ABSTRACT**

Nanofiltration has a pore size range of 0.001-0.01 $\mu$ m. NF membranes can filter particles up to and including some salts, synthetic dyes and sugars, however it is unable to remove most aqueous salts and metallic ions, as such, NF is generally confined to specialist uses. Nanofiltration (NF) is a promising membrane separation technology due to its low energy consumption and unique separation properties. The main objective of this research is to produce, characterize and evaluate performance of PES NF hollow fiber membrane for acetic acid removal from biomass hydrolyzate solution. An asymmetric PES hollow fiber membrane was fabricated using a dry/wet spinning process with forced convection in the dry gap. The PES concentration be fix at 20wt%, but the value of additive (PVP) is increase from 1wt% and 9wt.% and the rest is the value for NMP which act as solvent. The membranes were then analyzed by using scanning electron microscope (SEM) and high performance liquid chromatography (HPLC). Increase the concentration of PVP resulting decreased the rejection of the component it will increase the number of pore at the membrane and resulting in permeability of the membrane which increase of concentration of PVP will increase the permeability of the membrane. The increasing of additive concentration tends to increase the salt permeability while reducing the effective membranes thickness. In this case, the thickness of the effective membrane layer (dense layer) is very important and well known as one of the determining factors influencing the membranes separation ability.

Keywords: Nanofiltration membrane, Hollow fiber Module, Biomass



## **ABSTRAK**

Nanofiltration mempunyai pelbagai saiz liang 0.001-0.01 $\mu$ m. Membran NF boleh menapis zarah sehingga dan termasuk beberapa garam, mati sintetik dan gula, bagaimanapun ia tidak dapat menghapuskan garam akueus dan ion logam, oleh itu, NF biasanya terhad kepada pakar menggunakan. Nanofiltration (NF) adalah membran menjanjikan pemisahan teknologi kerana penggunaan tenaga yang rendah dan sifat pemisahan yang unik. Objektif utama kajian ini adalah untuk menghasilkan, mencirikan dan menilai prestasi PES NF serat berongga membran untuk penyingkiran asid asetik dari penyelesaian Hidrolisat biomass. Satu PES simetri membran gentian geronggang telah dibikin menggunakan proses berputar kering / basah dengan olakan paksa dalam jurang kering. PSB kepekatan akan menetapkan di 20wt%, tetapi nilai tambahan (PVP) adalah peningkatan daripada 1wt% dan 9wt.% Dan selebihnya adalah nilai untuk NMP yang bertindak sebagai pelarut. Membran kemudiannya dianalisis dengan menggunakan mikroskop imbasan elektron (SEM) dan kromatografi cecair prestasi tinggi (HPLC). Meningkatkan kepekatan PVP Hasilnya, Syarikat menurun penolakan komponen ia akan meningkatkan bilangan liang pada membran dan menyebabkan kebolehtelapan membran mana kenaikan penumpuan PVP akan meningkatkan kebolehtelapan membran. Peningkatan kepekatan tambahan cenderung meningkat kebolehtelapan garam di samping mengurangkan ketebalan membran yang berkesan. Dalam kes ini, ketebalan lapisan membran yang berkesan (lapisan padat) adalah sangat penting dan terkenal sebagai salah satu faktor yang menentukan mempengaruhi keupayaan membran pemisahan.

**Keywords:** membran Nanofiltration, Modul serat Hollow, Biomass

## TABLE OF CONTENTS

SUPERVISOR'S DECLARATION .....	IV
STUDENT'S DECLARATION .....	V
<i>Dedication</i> .....	VI
ACKNOWLEDGEMENT .....	VII
ABSTRACT.....	VII
ABSTRAK.....	VIII
TABLE OF CONTENTS .....	X
LIST OF FIGURES.....	XII
LIST OF TABLES .....	XIII
LIST OF ABBREVIATIONS.....	XIV
1 INTRODUCTION	1
1.1 Research Background	1
1.2 Objective of the Research	4
1.3 Scope of the Research	
2 LITERATURE REVIEW	5
2.1 Biomass	5
2.2 Biomass Processing	5
2.3 Membranes	7
2.3.1 Membrane Technology	10
2.4 Membrane Formation	11
2.5 Separation Technology for Inhibitor Removal	12
2.5.1 Extraction Process	12
2.5.2 Evaporation Process	14
2.5.3 Activated Charcoal Treatment	15
2.5.4 Ion Exchange Resins	15
3 METHODOLOGY	16
3.1 Dope Solution Preparation	16
3.2 Hollow Fibre Spinning	16
3.3 NF Cross Flow System	18
3.4 HPLC Analysis	19
3.4.1 Sugar Analysis	19
3.4.2 Acid Analysis	19
3.5 Scanning Electron Microscope (SEM)	20
4 METHODOLOGY	21
4.1 Morphology by SEM and Water Flux	21
4.2 Cross Flow Filtration	23
4.3 HPLC Analysis	24
4.3.1 Xylose and Glucose concentration	24
4.3.2 Acetic Acid	26
5 CONCLUSION AND RECOMMENDATION	25
5.1 Conclusion	25
5.2 Recommendation	25

REFERENCES	26
APPENDIX	31

## LIST OF FIGURES

Figure 2.1	Process for biomass	7
Figure 2.2	Schematic diagram of the basic membrane gas separation process	7
Figure 2.3	Schematic representation of different membrane morphologies; colored parts represent polymer	8
Figure 2.4	Cut-offs of different liquid filtration techniques.	10
Figure 2.5	Schematic representation of three DIPS processes	11
Figure 2.6	Flow diagram for extraction process	13
Figure 3.1	Schematic diagram for hollow fibre membrane production	17
Figure 3.2	Spinning Equipment used For Membrane Formation	17
Figure 3.3	U shaped cell membrane	18
Figure 3.4	Separation equipment use for filtration	19
Figure 4.1	Cross sectional photomicrographs of PES hollow fibers	22
Figure 4.2	Normalized flux for membrane A and B	24
Figure 4.3	Peak and area for xylose and glucose from HPLC analysis	24
Figure 4.4	Calibration curve for xylose and glucose	25
Figure 4.5	Peak and area for acetic acid from HPLC analysis	26
Figure 4.6	Calibration curve for acetic acid	27
Figure 4.7	Percentage of rejection for xylose in different concentration of NMP	31
Figure 4.8	Percentage of rejection for glucose in different concentration of NMP.	31
Figure 4.9	Percentage of rejection for acetic acid in different concentration of NMP	32
Figure 4.10	Graph of percentage for rejection of hydrolyzate in different concentration of PVP	33

## LIST OF TABLES

Table 2.1	Properties of xylose, glucose and acetic acid	6
Table 2.2	Pressure driven processes using porous membranes ( J. A. van't et. al, 1992)	9
Table 3.1	Composition, flowrate and time use for one rotation for each solution.	18
Table 4.1	Permeability for each membrane A and B	23
Table 4.2	Concentration obtain from separation for membrane A ( 20wt% PES,1wt% PVP and 79 wt% NMP)	28
Table 4.3	Concentration obtain from separation for membrane B ( 20wt% PES,9 wt% PVP and 71 wt% NMP)	28
Table 4.4	Concentration obtain from separation for membrane A ( 20wt% PES,1wt% PVP and 79 wt% NMP) in hydrolysate solution	29
Table 4.5	Concentration obtain from separation for membrane B ( 20wt% PES,9wt% PVP and 71 wt% NMP) in hydrolysate solution.	29
Table 4.6	Flux of concentration at pressure 5 bar (L/m <sup>2</sup> .h.bar)	30
Table 4.7	Rejection value of xylose, glucose and acetic acid for each concentration of PVP	30
Table 4.7	Rejection value of xylose, glucose and acetic acid in hydrolysatefor each concentration of PVP	32

## LIST OF ABBREVIATIONS

$A_0$	constant of eq.(3.6)
$A_s$	constant of eq.(3.6)
$a$	interfacial area per unit volume
$a(L_i)$	breakage kernel
$b(k, L_i)$	daughter bubble distribution function
$B$	nucleation kernel
$C$	impeller off-bottom clearance
$C_o^*$	oxygen solubility in water
$C_D$	drag coefficient
$v_g$	superficial gas velocity
$VVM$	volume per unit volume
$w$	weight
$W$	impeller blade width
$Y_v$	turbulent destruction term for Spalart-Almaras model

### *Greek*

$\nu_l$	kinematic viscosity
$\theta_{ie}$	collision rate of bubbles with turbulent eddies
$\kappa_i$	break-up efficiency
$\Lambda(L_i, L_j)$	bubble collision efficiency

### *Subscripts*

$b$	bubble
$g$	gas
$l$	liquid
$eff$	effective

## LIST OF ABBREVIATIONS

CARPT	Computer-automated radioactive particle tracking
CFD	Computational fluid dynamics
CSP	Capillary suction probe
CT	Computer tomography
DAE	Differential algebraic equation
DES	Detached eddy simulation
DI	Digital imaging
EIT	Electric impedance tomography
ERT	Electric resistance tomography
FFT	Fast Fourier transform
GRT	Gamma ray tomography
IZ	Ishii-Zuber drag model
LDA	Laser doppler anemometry
LES	Large eddy simulation
LIF	Laser image fluorescence
MOC	Method of classes
MOCh	Method of characteristic
MOM	Method of moment
MRF	Multiple reference frame
PD	Product difference
PBE	Population balance equation
PBM	Population balance modelling
PDA	Phase doppler anemometer
PIV	Particle image velocimetry
PLIF	Planar laser induced fluorescence
QMOM	Quadrature method of moment
RDT	Rushron turbine
RANS	Reynolds averaged Navier-Stokes
RNG	Renormalised $k$ - $\epsilon$
RSM	Reynolds stress model
SA	Spalart-Allmaras model
SGS	sub-grid scale
SMM	Sliding mesh method
SN	Schiller-Naumann drag model
SST	Shear stress transport model

# 1 INTRODUCTION

## 1.1 Research Background

Lignocellulosic materials such as agricultural, hardwood and softwood residues that produced bioethanol is a promising alternative energy because lignocellulosic materials do not compete with food crops. In a typical bioconversion process to produce “second generation” bioethanol, the hemicellulose is converted to pentose (predominately xylose) by hydrolysis pre-treatments, while the cellulose is converted to hexose (predominately glucose) by enzymatic hydrolysis. After hydrolysis process, these sugars can be fermented and converted to ethanol (Chen et al., 2011)

However, the by-products such as furans, carboxylic acid and phenolic substances, were also generated in the hydrolysis process, which can significantly suppress fermentative organisms and decrease the ethanol yield and productivity. Acetic acid, one of the inhibitors, which was studied in detail due to its highest content in hydrolyzates, is generated by the hydrolysis of the acetyl group on hemicellulose and is commonly observed along with the release of xylose (Mussatto and Robert, 2004). With the presence of acetic acid in high concentration, the growth of fermentation microorganisms and the production of ethanol are strongly affected (Palmqvist and Hahn-Hagerdal B., 2000)

There are several methods to remove acetic acid including dehydration of acetic acid, filtration by membrane and so on. Nevertheless, the application of membrane separation in bio-energy studies, especially for acetic acid removal, is still in the early stages. Pressure-driven membrane processes have drawn great attention in the industry for their unique ability to separate and purify products from process streams including microfiltration (MF), ultrafiltration (UF), nanofiltration (NF) and reverse osmosis (RO). Applications of NF to the separation, purification and concentration of products from streams have been emerging in various fields, including fermentation product separation, sugar fractionation and sugar concentration (Weng, 2009)



By using nanofiltration membrane, the observed retention of xylose and acetic acid varied from 28% to 81% and  $-6.8\%$  to 90%, respectively, depending on the solution pH and the applied pressure. The maximum separation factor was 5.4 when the system was operated at pH 2.9 and 24.5 bar. In addition, negative retention of acetic acid was observed only in the presence of xylose. The results suggested that intermolecular interactions play an important role in the separation of xylose and acetic acid (Weng, 2009).

The high demands of sustainable alternative transportation fuels are of interest as second-generation biofuels. One type biofuel is ethanol produced from non-food biomass. It is necessary to increase the ethanol concentration of the product after fermentation to decrease the energy required for the final separation process and to commercialize lignocellulosic ethanol technology. In order to increase the yield of ethanol, acetic acid should be extracted from the enzymatic hydrolyzates because the present of acetic acid limited the production of ethanol. Concentrating enzymatic hydrolyzates which are glucose and xylose using membrane separation process, nanofiltration, with molecular weight cut offs between ultrafiltration and reverse osmosis, is attractive because nanofiltration is a widely used technique in biorefineries due to its low energy consumption and unique separation properties. Membrane is very important part to remove the acetic acid and increase the concentration of glucose and xylose.

Membrane filtration is an efficient, cost-competitive and promising separation method during industrial production process (Pinelo et al., 2009). Applications of membrane technology for, sugar concentration, sugar fractionation, and inhibitor separation from lignocellulose hydrolyzates were studied in recent years. Murthy et al. reported the concentration of xylose reaction liquor can be effectively accomplished by nanofiltration, while Sjöman et al. found that the xylose purification from hemicellulose hydrolyzates could be enhanced by nanofiltration. As the inhibitor with the highest content in hydrolyzates, acetic acid was firstly separated by Han and Cheryan from an acetic acid–glucose model solution by using NF and RO membranes, and acetate rejection of 40% and glucose rejection of 99% were obtained, respectively. Sagehashi et al. employed RO membranes to separate phenols and furfural from the aqueous solution derived from the superheated steam pyrolysis of biomass, and the solution was

concentrated effectively by reverse osmosis separation. Several researchers also reported the separation of carboxylic acids or furans from sugars in dilute-acid hydrolyzates or fast pyrolysis bio-oils by using NF or RO membranes (Qi et al., 2011; Teella et al., 2011; Weng et al., 2009, 2010).

Applications of NF to the separation, purification and concentration of products from streams have been emerging in various fields, such as fermentation product separation (Han I. S,1995) sugar fractionation (Sjoman E. , 2007) and sugar concentration (Murthy G.S., 2005) In general, NF can distinguish molecules via sieving effect as well as by charge effect. The retention of uncharged molecules by NF will be determined mainly by sieving effects. Molecules with a molecular weight larger than that of the sieving characteristics or exclusion properties of the NF membrane would be rejected.

The separation of multi-valent ions by NF is high due to the Donnan effect. Han and Cheryan were the first to study the separation of sugar from acetic acid. They found the pH is a major factor influencing the separation of acetic acid from glucose. More recently, Sjoman et al. studied the separation of xylose from glucose via commercially available in NF membranes. Murthy et al. reported that concentration of xylose by NF from 2% to 10% (w/v) was successful separated in a pilot plant. In addition, they found the operational costs for xylose concentration by NF were one-fourth that of a conventional evaporation process. Although solution pH is an important factor governing NF performance, the effect of solution pH on the separation performance was not explored in their pilot plant study. To the best of my knowledge, there were only a few investigations on NF separation of acetic acid from monosaccharide except for some studies on downstream processing of acetate by NF after glucose fermentation. Furthermore, there is limited information on the purification of xylose for bioethanol production.

In this study, acetic acid was separated using nanofiltration hollow fibre membrane from xylose and glucose by using different concentration of NMP. Constant pressure was apply while separation to investigate the result of separation of acetic acid from xylose and glucose. From the literatures, NF was concluded as the standard membrane process for acetic acid separation from sugars, due to the negative retention

of acetic acid. Zhou et al., have mentioned the membrane performance of NF and RO membrane for acetic acid separation from monosaccharaides was compared in a comprehensive manner.

## **1.2 Objective of the Research**

The main objective of this research is to produce, characterize and evaluate performance of Polyethersulfone (PES) NF hollow fiber membrane for acetic acid removal from synthetic biomass hydrolysate solution.

## **1.3 Scope of the Research**

In order to fulfill the research objective, the following scopes has been outlined.

- i. To produce two different composition of NF hollow fiber membrane A (20 wt% PES, 1wt% PVP, and 79 wt% NMP) and B (20 wt% PES, 9wt% PVP, and 71 wt% NMP)
- ii. To characterize and evaluate the performance of PES NF hollow fiber membrane using pure solution ( xylose, glucose and acetic acid ) and synthetic hydrolyzate solution ( i.e. mixture of xylose, glucose and acetic acid )

## **2 LITERATURE REVIEW**

### **2.1 Biomass**

Biomass simply define as all plant material, or vegetation, raw or processed, wild or cultivated. Examples of this energy source include fast growing trees and grasses, agricultural residues like used vegetable oils, wheat straw, or corn, yard clippings , wood waste like paper trash, sawdust, or wood chips, and methane that is captured from landfills, livestock, and municipal waste water treatment. Essentially, biomass is stored solar energy that human can convert to electricity, fuel, and heat. The energy from the sun is stored in the chemical bonds of the plant material through photosynthesis. Typically biomass energy comes from three sources for example agricultural crop residues, municipal and industrial waste, and energy plantations. In addition, crops such as corn, sugar beets, grains, and kelp can be grown specifically for energy generation. Table below shows the properties xylose, glucose and acetic acid.

### **2.2 Biomass Processing**

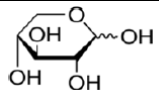
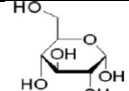
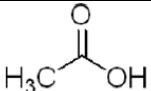
Biomass goes through a size-reduction step to make it easier to handle and to make the ethanol production process more efficient. Figure 2.1 shows the biomass process. For example, agricultural residues go through a grinding process and wood goes through a chipping process to achieve a uniform particle size. Biomass is then being treated. In this step, the hemicellulose fraction of the biomass is broken down into simple sugars. A chemical reaction called hydrolysis occurs when dilute sulphuric acid is mixed with the biomass feedstock. In this hydrolysis reaction, the complex chains of sugars that make up the hemicellulose are broken, releasing simple sugars. The complex hemicellulose sugars are converted to a mix of soluble five-carbon sugars, xylose and arabinose, and soluble six-carbon sugars, mannose and galactose. Table 2.1 show the properties of xylose, glucose and acetic acid. Acetic acid, one of the inhibitors, which was studied in detail due to its highest content in hydrolyzates, is generated by the hydrolysis of the acetyl group on hemicellulose and is commonly observed along with

the release of xylose. The presence of acetic acid can limited the production of ethanol during fermentation process.

Production of ethanol from lignocellulose has the advantage of abundant and diverse raw material compared to sources such as corn and cane sugars, but requires a great amount of processing to make the sugar monomers available to the microorganisms typically used to produce ethanol by fermentation. Switchgrass and *Miscanthus* are the major value of biomass materials being studied today, due to their high productivity per acre. Cellulose, is contained in nearly every natural, free-growing plant, tree, and bush, in meadows, forests, and fields all over the world without agricultural effort or cost needed to make it grow. One of the benefits of cellulosic ethanol is it reduces greenhouse gas emissions.

Absence of production of cellulosic ethanol in the quantities required by the regulation was the basis of a United States Court of Appeals for the District of Columbia decision announced January 25, 2013 voiding a requirement imposed on car and truck fuel producers in the United States by the Environmental Protection Agency requiring addition of cellulosic biofuels to their products. These issues, along with many other difficult production challenges, lead George Washington University policy researchers to state that "in the short term, [cellulosic] ethanol cannot meet the energy security and environmental goals of a gasoline alternative."

**Table 2.1** Properties of xylose, glucose and acetic acid

Component	Xylose	Glucose	Acetic Acid
Molecular formula	C <sub>5</sub> H <sub>10</sub> O <sub>5</sub>	C <sub>6</sub> H <sub>12</sub> O <sub>6</sub>	CH <sub>3</sub> COOH
Molecular Structure			
Molecular Weight (gmol <sup>-1</sup> )	150.13	180.156	60.05
Stokes diameter (nm)	0.638	0.726	0.412
Diffusion coefficient (cm <sup>2</sup> s <sup>-1</sup> )	7.69	6.76	11.9

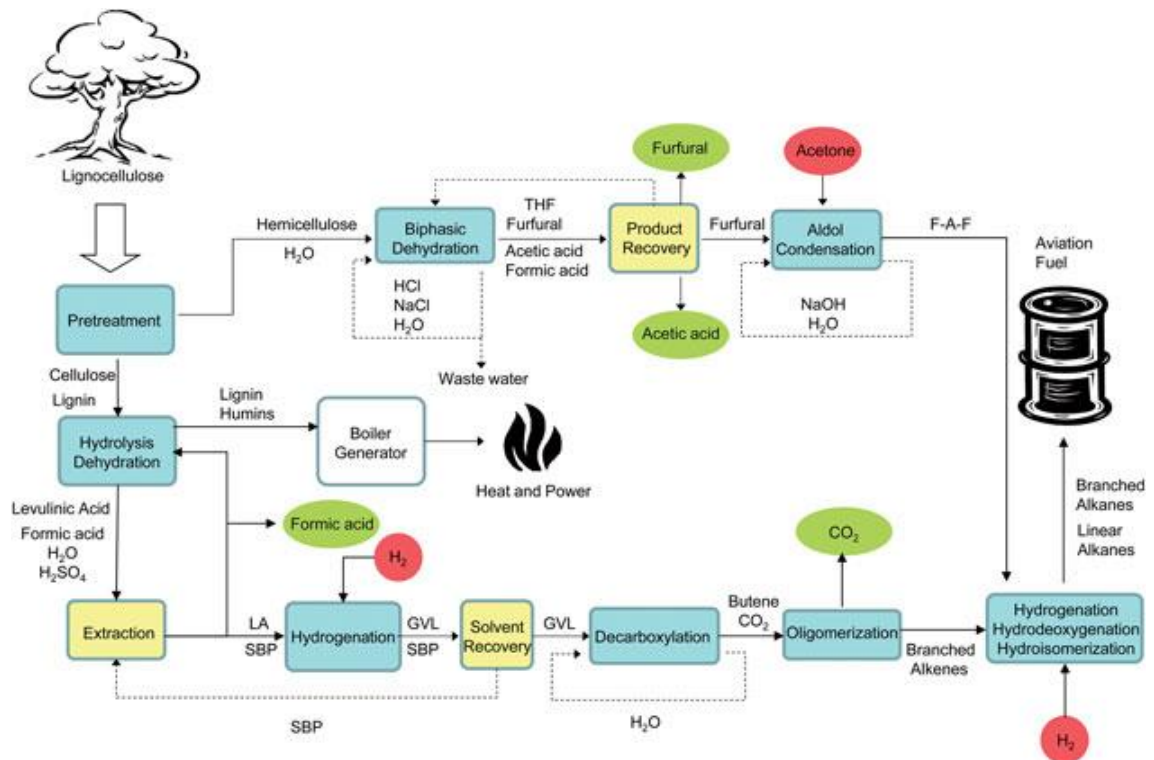


**Figure 2.1** Process for biomass.

## 2.3 Membranes

A membrane can be defined essentially as a barrier, which separates two phases and restricts transport of various chemical species in a selective manner as shown in Figure 1. The stream that retained by the membrane is the retentate while the one permeates through the membrane is the permeate stream. Either of the two streams retentate or permeate could be the end-use products in a membrane-based separation process (Mulder, 1996). The selectivity of membrane is due to its size, physicochemical interactions, shape, electrostatic charge, diffusivity, volatility and polarity/solubility.

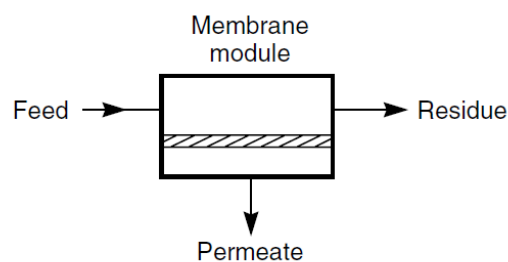


**Figure 2.2:** Schematic diagram of the basic membrane gas separation process

There are 4 types of membrane module which are plate-and-frame, tubular, spiral wound and hollow fiber. Membrane separation by using hollow fibers has become the one of emerging technologies which underwent a rapid growth during the past few decades. The excellent mass-transfer properties conferred by the hollow fiber configuration led to the numerous commercial applications in various fields such as the medical field (blood fractionation), water reclamation (purification and desalination), ultrafiltration, microfiltration, liquid/liquid or liquid/solid separation, reverse osmosis, gas separation, hemodialysis, removal of VOCs from water and so on (Feng, 2013).

Through this definition, a membrane should always be associated with its application. There are several application of membrane include desolation, dialysis and also filtration to gas separation. Different membrane morphologies will be used depending on the application. In figure 2.2, a schematic representation of different morphologies is given.

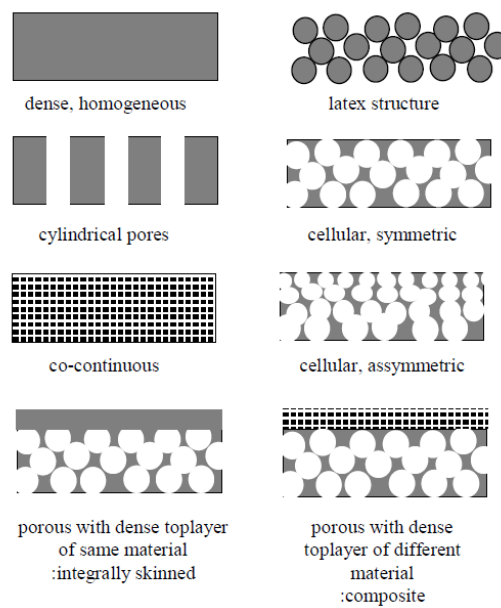


**Figure 2.3** Schematic representation of different membrane morphologies; colored parts represent polymer.

There are several types of membrane separation mechanisms exist. In membrane applications, the sorption-diffusion mechanism plays the major role where the choice of the membrane material is based on selective sorption and diffusion properties.

Membrane morphology will not play a major role in issues of selectivity but they do with total flux. For examples of these applications is gas separation, pervaporation and reverse osmosis. The second separation mechanism is based on the size of the species to be separated. Membranes will have typically pore sizes that can give rise to retention of certain species. In table 1.1, the pore sizes of the different membrane categories are given. Besides average pore size and pore size distribution, other parameters like or electrical charge can have a large influence too on its separation characteristics. These membranes are often used in pressure driven processes.

**Table 2.2 :** Pressure driven processes using porous membranes ( J. A. van't et. al, 1992)

<b>Membrane application</b>	<b>Pore size</b>	<b>Typical flux (l/m<sup>2</sup>.h.bar)</b>	<b>Typical Pressure (bar)</b>	<b>Examples of materials retained</b>
Microfiltration	>50nm	>50	0.1-2	Particles (bacteria, yeast)
Ultrafiltration	1nm – 100 nm	10-50	1-5	Macromolecules, colloids
Nanofiltration	≈1 nm	1.4-12	5-20	Solutes Mw > 500, multivalent ions
Reverse Osmosis	Non porous	0.005-1.4	10/100	water

The structure or morphology of the membrane will have an effect on the total flux through the membrane. Decreasing the total thickness of the membranes would therefore be advantageous. However, this is limited due to mechanical stability constraints. This is overcome by preparing asymmetric membranes in which the separating part of the membrane is situated in a thin layer of the membrane. The majority of the structure will only serve as a mechanical support for this selective layer. The selective layer and mechanical support of membranes must be optimized.



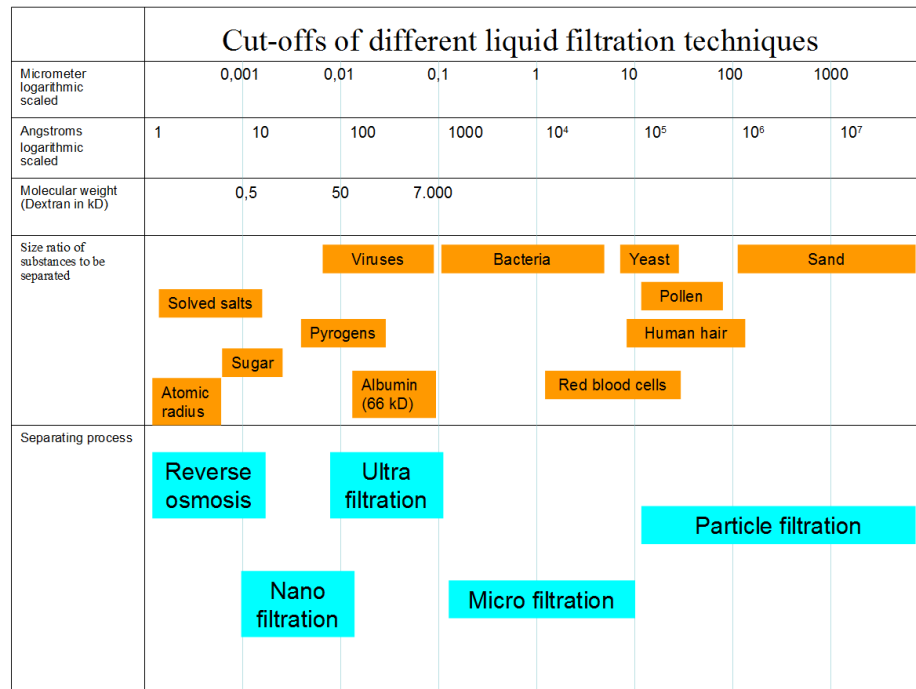


**Figure 2.4:** Cut-offs of different liquid filtration techniques.

### 2.3.1 Membrane Technology

Membrane technology has become a dignified separation technology over the past decennia. The main force of membrane technology is the fact that it works without the addition of chemicals, with a relatively low energy use and easy and well-arranged process conductions. Membrane technology is a generic term for a number of different, very characteristic separation processes. These processes are of the same kind, because in each of them a membrane is used. Membranes are used more and more often for the creation of process water from groundwater, surface water or wastewater. Membranes are now competitive for conventional techniques. The membrane separation process is based on the presence of semi permeable membranes. The principle is quite simple: the membrane acts as a very specific filter that will let water flow through, while it catches suspended solids and other substances. There are various methods to enable substances to penetrate a membrane. Examples of these methods are the applications of high pressure, the maintenance of a concentration gradient on both sides of the membrane and the introduction of an electric potential.

## 2.4 Membrane Formation

During the three decades of intensive membrane preparation research, different techniques have been proposed to generate selective, permeable films. The most used and thus important class of techniques is called phase inversion techniques. These processes rely on the phase separation of polymer solutions producing porous polymer films. Phase separation mechanisms can generally be subdivided in three main categories depending on the parameters that induce demixing which are temperature induced phase separation (TIPS), reaction induced phase separation (RIPS) and diffusion induced phase separation (DIPS). By posing a change in one of these parameters at one particular side of the film, asymmetric boundaries are posed on the polymer film which can be expressed in the resulting structure. By changing the temperature at the interface of the polymer solution, heat will be exchanged and demixing can be induced (temperature induced phase separation or TIPS). The original polymer solution can also be subjected to a reaction which causes phase separation (reaction induced phase separation) (RIPS). The most used technique is based on diffusion induced phase separation (DIPS). By contacting a polymer solution to a vapour or liquid, diffusional mass exchange will lead to a change in the local composition of the polymer film and demixing can be induced.

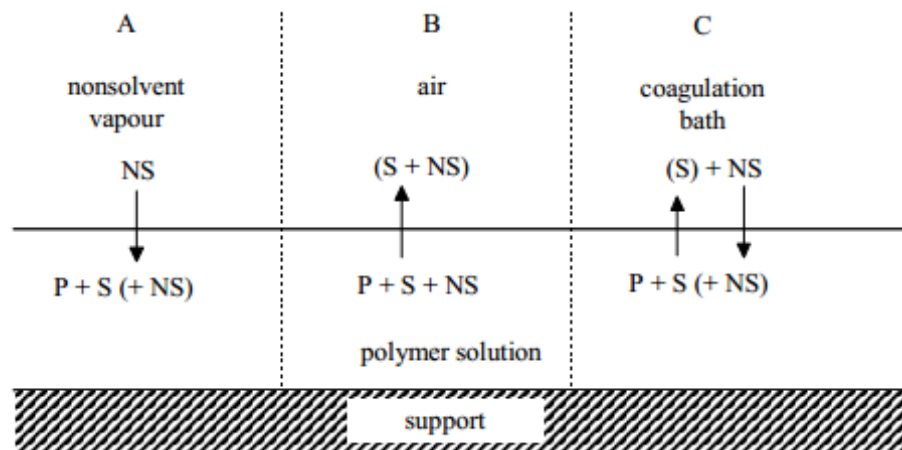


**Figure 2.5** Schematic representation of three DIPS processes: A) precipitation with nonsolvent vapor, B) evaporation of solvent, C) immersion precipitation. Main direction of diffusion of the different species is indicated by arrows. Polymer, solvent and nonsolvent are represented with P, S and NS respectively.

Three types of techniques were developed to reach DIPS: coagulation by absorption of nonsolvent from a vapor phase, evaporation of solvent and immersion into a nonsolvent bath. These techniques are schematically represented in figure 2.3. Often combinations of various techniques are made to achieve the desired membrane. When a polymer is subjected to a vapor containing a nonsolvent (a species not miscible with the polymer), often symmetric structures are generated. Membrane formation by evaporation (porous structures) uses polymer solutions containing a volatile solvent, a less volatile nonsolvent and a polymer. Preferential loss of solvent will generate meta- or unstable compositions and phase separation will be induced at this point. Immersion precipitation is achieved by diffusion of nonsolvent from a coagulation bath into the polymer film and diffusion of solvent from the polymer solution into the nonsolvent bath. Although the processes are quite easy to perform, the exact conditions under which a particular membrane will be formed is often derived on empirical grounds.

## **2.5 Separation Technology For Inhibitor Removal**

Acetic acid, one of the inhibitors, which was studied in detail due to its highest content in hydrolyzates, is generated by the hydrolysis of the acetyl group on hemicellulose and is commonly observed along with the release of xylose. The growth of fermentation microorganisms and the production of ethanol are strongly affected by the presence of acetic acid in high concentration. In order to separate acetic acid from hydrolyzates, biological, physical, and chemical methods as well as combined treatments have been employed for example detoxification method including microbiology, vacuum evaporation, extraction, overliming, activated charcoal adsorption, and ion exchange.

### **2.5.1 Extraction process**

Extraction plant consists of the extraction tower, the rectification tower for the recovery of the extraction agent, and the water-stripping tower. As a rule, the feed mixture has a greater density than the solvent, and is fed in at the top end of the

extraction tower. Inside the tower it streams towards the bottom and in the process gives off acetic acid to the extraction agent. Depending on the effort, residual concentrations of 0.1-0.5 wt% can be achieved. Since the aqueous phase is simultaneously saturated with the extraction agent in the extraction tower, it is recovered in a downstream stripping tower. It can in this respect be performed with live steam. The extraction agent accumulates at the top end of the rectification tower and the acetic acid at the bottom of the tower resulting in acetic-acid concentrations of practically 100 wt%. If there is a risk of any higher-boiling components also passing into the organic phase during extraction, then it is recommended that the acetic acid should be discharged in vapor form.

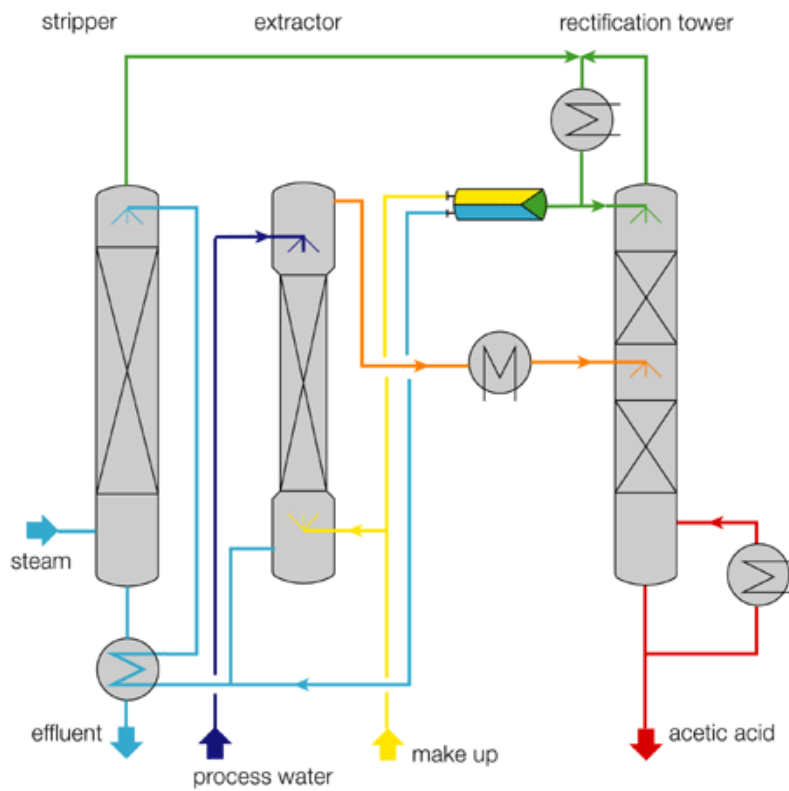


**Figure2.6** Flow diagram for extraction process

### 2.5.1 Evaporation Process

Evaporation is a simple procedure to remove acetic acid, furfural and other volatile components in the hydrolyzates. However, this method retains the concentration of non-volatile toxic compounds (extractives and lignin derivatives) in the hydrolyzates. Palmqvist et al., (1996) observed the removal of most volatile fraction (10% v/v) from willow hemicellulose hydrolyzate by roto-evaporation. Wilson et al., (1989) found a decrease in the concentration of acetic acid, furfural and vanillin by 54%, 100% and 29%, respectively, compared with the concentrations in the hydrolyzate. Larsson et al., (1999) observed the removal of furfural (90%) and HMF (4%) using vacuum evaporation from wood hemicellulosic hydrolyzate. For instance, Converti et al.(2000) hydrolyzed the *E. globules* wood by steam explosion and dilute acid treatment at 100 °C, followed by boiling or evaporating the obtained hydrolyzate for 160 min to decrease the concentration of acetic acid and furfural from 31.2 to 1.0 g/l and from 1.2 to 0.5 g/l, respectively. These are below their inhibitory levels for the fermentation of xylose to xylitol by *Pachysolen tannophilus* strain, showing that in this case the simple evaporation method is sufficient to eliminate the inhibition of acetic acid and furfural. Solvent extraction with ethyl acetate is effective to remove all of the inhibitory compounds except for the residual acetic acid (Wilson et.al,1989) e.g. ethyl acetate extraction can be used to remove 56% acetic acid and all of furfural, vanillin, and 4-hydroxybenzoic acid (Palmqvist, 2000). Solvent extraction with ethyl acetate is effective to remove all of the inhibitory compounds except for the residual acetic acid (Wilson et.al,1989) ,e.g. ethyl acetate extraction can be used to remove 56% acetic acid and all of furfural, vanillin, and 4-hydroxybenzoic acid (Palmqvist, 2000)

Another potential substrate sugarcane bagasse was hydrolyzed and vacuum evaporated followed by activated charcoal treatment, revealed 89% removal of furfural (Rodrigues et al., 2001) with partial elimination of acetic acid. Zhu et al., (2011) applied the complex extraction to detoxify the prehydrolysate corn stover using mixed extractant (30% trialkylamine-50% n-octanol–20% kerosene). The detoxification resulted into removal of 73.3% acetic acid, 45.7% 5-HMF and 100% furfural.

## 2.5.2 Activated Charcoal Treatment

The detoxification of hemicellulose hydrolysates, by activated charcoal is known to be a cost effective with high capacity to absorb compounds without affecting levels of sugar in hydrolysate (Canilha et al., 2008; Chandel et al., 2007). The effectiveness of activated charcoal treatment depends on different process variables such as pH, contact time, temperature and the ratio of activated charcoal taken versus the liquid hydrolysate volume (Prakasham et al., 2009).

## 2.5.3 Ion Exchange Resins

Treatment with ion exchange resins has been known to remove lignin-derived inhibitors, acetic acid and furfurals respectively, leading to hydrolysate that show a fermentation similar to that of an inhibitor-free model substrate. The ion-exchange resins based separation of fermentative inhibitors may not be cost effective (Lee et al., 1999), however, it provides most effective means of inhibitor separation when the hydrolyzate being adjusted to a pH of 10 which requires significant quantities of base chemicals (Wilson and Tekere, 2009). Further, the anion treatment also helps to remove most inhibitors (i.e. levulinic, acetic, formic acids, and furfural and 5-HMF).

The effect of four different ion exchange resins (cation and anion) was investigated for the detoxification of *Eucalyptus* hemicellulosic hydrolysates for the improved xylitol production by *Candida guilliermondii* (Villarreal et al., 2006). The ion exchange detoxification drastically enhanced the fermentability of the hydrolyzate. Total 32.7 g/l of xylitol was achieved after 48 h fermentation, which correspond to 0.68 g/l/h volumetric productivity and 0.57 g/g xylitol yield factor (Villarreal et al. 2006). The ion exchange resins also led to a considerable loss of fermentable sugars from the hydrolyzate. Chandel et al. (2007) observed that ion exchange resins diminish furans (63.4%) and total phenolics (75.8%) from sugarcane bagasse acid hydrolysates. Although the ion exchanges resins is effective, however is not cost effective that reflects its limited feasibility in commercial industrial purpose in lignocellulosics derived products synthesis.

### **3 METHODOLOGY**

#### **3.1 Dope Solution Preparation**

20 wt % of Polyethersulfone (PES) was weight and mix into 79 wt% of N-methyl-2-pyrrolidone (NMP) with 1 wt% of Poly-Vinylchloride (PVP) under 60 °C hotplate by continuous stirring. Another dope solution was make using 9wt% PVP and 71wt% NMP.

#### **3.2 Hollow Fibre Spinning**

An asymmetric PES hollow fiber membrane is fabricated using a spinning process with forced convection in the dry gap. On extrusion from the spinneret, the dope solution being push by hydrogen gas passed through a spinneret with 0.8mm ID and 1.4mm OD. The spinning was run with 8cm air gap. Water was use as coagulation medium and the spinning was run. The prepared membranes were immersed in a copious amount of water over a couple of days to remove the solvent and bore fluid from the membranes. The membrane was then air dried.

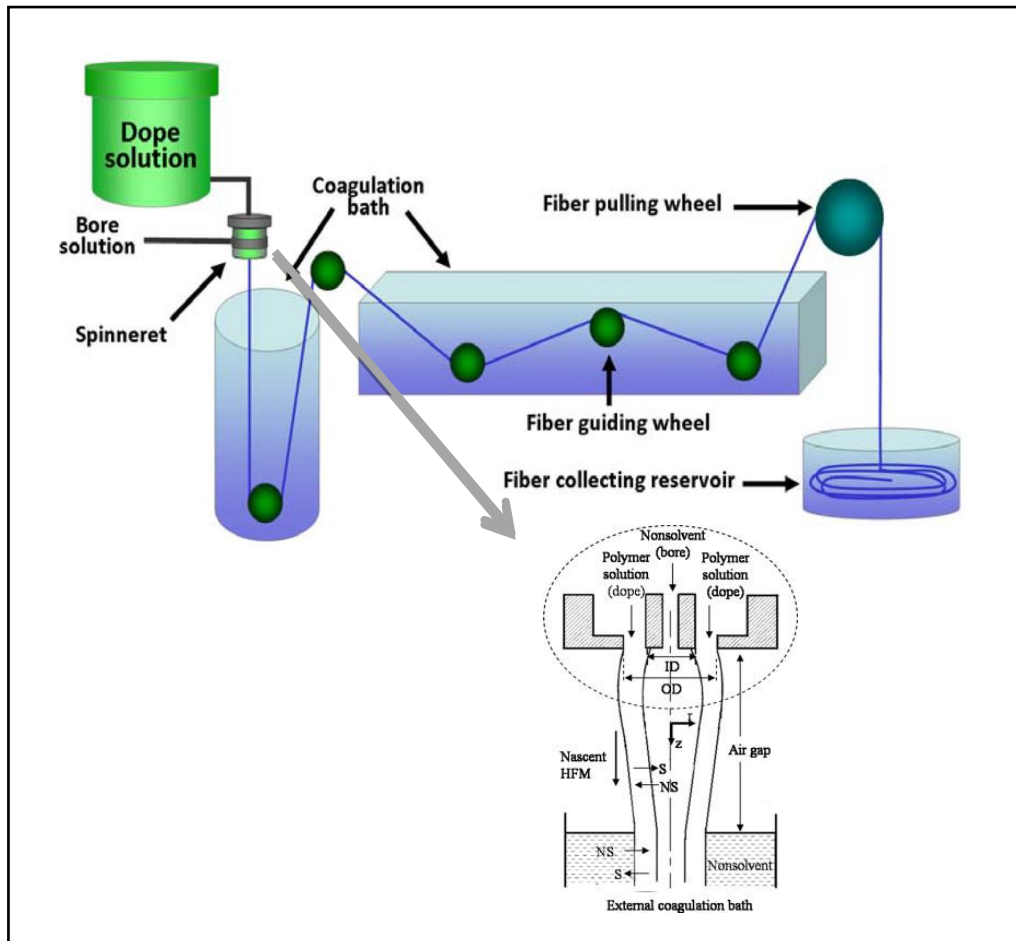


**Figure 3.1** Schematic diagram for hollow fibre membrane production.



**Figure 3.2** Spinning Equipment used For Membrane Formation



### 3.3 NF Cross Flow System

Dried membrane was module before separation process. The membrane was module using U shaped cell membrane. Figure shows the shape of our module. 15-30 hollow fiber membrane was used in module development. PVC was used as the tube for the module. The module was then connecting in cross flow system. 4 modules were produce for each membrane A and B to get the average value of After the pure water flux and salt retention tests, 2 L model solution was added in the feed tank, and then the feed solution was circulated through the system until the experimental conditions were stable. The filtration of model solutions was done in total recirculation mode, i.e. both permeate and retentate were recycled back to the feed tank. Small amount of samples (1 mL) were taken from permeate and retentate for chemical analysis during the experiment. The filtration pressures used were 5 bar which were lower than the maximum allowed pressures for each membrane. For each experimental condition, flux was measured twice to obtain an average value.

**Table 3.1:** Composition, flowrate and time use for one rotation for each solution.

<b>Hollow Fibre</b>	<b>Composition (wt%) (PES:PVP:NMP)</b>	<b>Water flowrate (m<sup>3</sup>/min)</b>	<b>Rotation (m/s)</b>	<b>Air gap (cm)</b>
<b>A</b>	20:1:79	$5.329 \times 10^{-6}$	11.44	8
<b>B</b>	20:9:71	$4.553 \times 10^{-6}$	11.70	8



**Figure 3.3** U shaped cell membrane



**Figure 3.4** Separation equipment use for filtration

## **3.4 HPLC Analysis**

### **3.4.1 Sugar Analysis**

Xylose and glucose were quantified by the high performance liquid chromatography (HPLC) system using a 4.6 mm x 250 mm High Performance Carbohydrate column. Degassed, Acetonitrile and water with ratio 75:25 (v/v) was used as mobile phase. The column temperature was maintained at 80 °C and the flow rate for the mobile phase was fixed at 0.6 ml/min. Peaks were detected by the refractive index (RI) detector and quantified on the basis of area and retention time of the sugar standards.

### **3.4.2 Acid Analysis**

Acetic acid was estimated by HPLC using a Biorec HPX column at 65 °C using 0.004N of Sulfuric Acid as mobile phase at a flow rate of 0.6 ml/min. Peaks were detected by the refractive index (RI) detector and quantified on the basis of area and retention time of the sugar standards.

### **3.5 Scanning Electron Microscope (SEM)**

The cross-sections of membranes morphology of Nanofiltration membranes were observed using scanning electron microscope. For this purpose, the membrane samples were dried and then fractured cryogenically in liquid nitrogen before mounting on sample stubs. The samples were then sputtered with a thin layer of gold using a sputtering apparatus. After gold sputtering, the samples were examined with electron microscope.

## **4 RESULT AND DISCUSSIONS**

### **4.1 Morphology by SEM and water Flux**

The effect of PVP on the formation of membranes was studied extensively by several authors. The performances of ultrafiltration membranes by Lafreniere et al. Han and Nam have also conducted study on the effect of water-soluble additive on the morphological structure of asymmetric membranes. PVP should increase the membranes hydrophilicity when PVP is entrapped by membranes materials (Marchese et al , 2003) and also resulted in the alteration of ultrafiltration membranes performance in terms of solute rejection and fouling phenomenon. Furthermore, it has been known that the addition of PVP in the polymer solution could be controlled in order to form the best morphological membranes structure.

In this case, the amount of residual or dissolution of PVP causes an increase in the number of membrane pore size and pore size distribution. Figure 4.0 shows the SEM photographs of cross-sectional images of PES membranes at different PVP concentration ranges of 1wt% and 9wt%. As we can see from the figures, both membranes show almost same morphology which consist of finger-like macrovoids in the inner and outer structure. It is based on the composition of PVP in each solution of membrane. This means that increasing of PVP concentration in the polymer solution causes reduction of membranes effective skin layer and also enhances the number of formation for membranes pore and pore size distributions.

The fact that increasing of additive concentration tends to increase the number of membrane pore has been proven and obviously shown by the membranes cross-sectional structure. As PVP is increased, the number of membranes pore was also found to increase which in turn resulted in higher flux and lower rejection. In fact, the change of membranes morphological structure by addition of additives is quite noticeable. In addition, the number of macrovoids was also found to disappear gradually as PVP concentration is increased. It is reported that the addition of PVP, which is frequently used as pore former additive, could induce the formation of finger-like structures and macrovoids both at the outer and the inner surfaces.

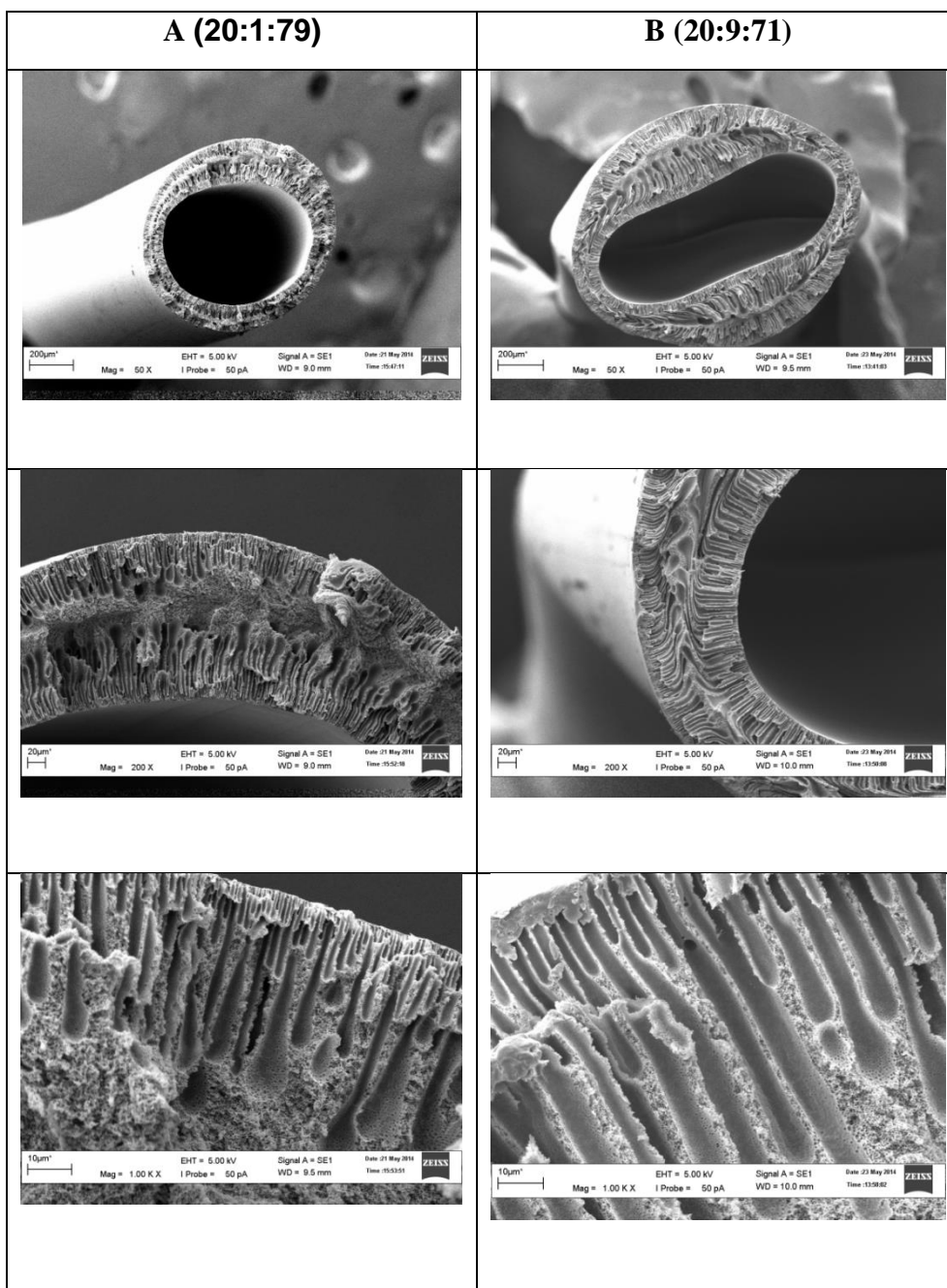


**Figure 4.1** Cross sectional photomicrographs of PES hollow fibers prepared at different composition A (20 wt% PES, 1 wt% PVP and 79 wt% NMP) and B (20 wt% PES, 9 wt% PVP and 71 wt% NMP)

## 4.2 Cross Flow Filtration

**Table 4.1** Permeability for each membrane A and B

<b>SAMPLE</b>	<b>A</b>	<b>B</b>
PES:PVP:NMP (wt%)	20:1:79	20:9:71
Area (m <sup>2</sup> )	26.39 x10 <sup>-3</sup>	19.792x10 <sup>-3</sup>
Normalizes Flux (L/m <sup>2</sup> .h.bar)	0.412	119.723

Table 3.0 shows dope formulation for the asymmetric PES nanofiltration membranes produced in this study. In order to study the influence of additive concentration on the NF performance, membrane morphology and structural parameters, two dope formulations have been prepared by varying of PVP concentration were 1.00 and 9.00 wt%. Using a U shaped cell, the membrane performance which is described in terms of flux and salt rejection was tested under operating pressure of 5 bar. The permeation experiment was performed using 5g/L for each xylose, glucose, acetic acid and also hydrolyzate solutions. Based on Fig. 1, the experimental data showed that the membrane permeability was increased as the PVP concentration is gradually increased. From the literature, membrane permeability increase as the PVP concentration increase and resulted in the reduction of salt rejection.

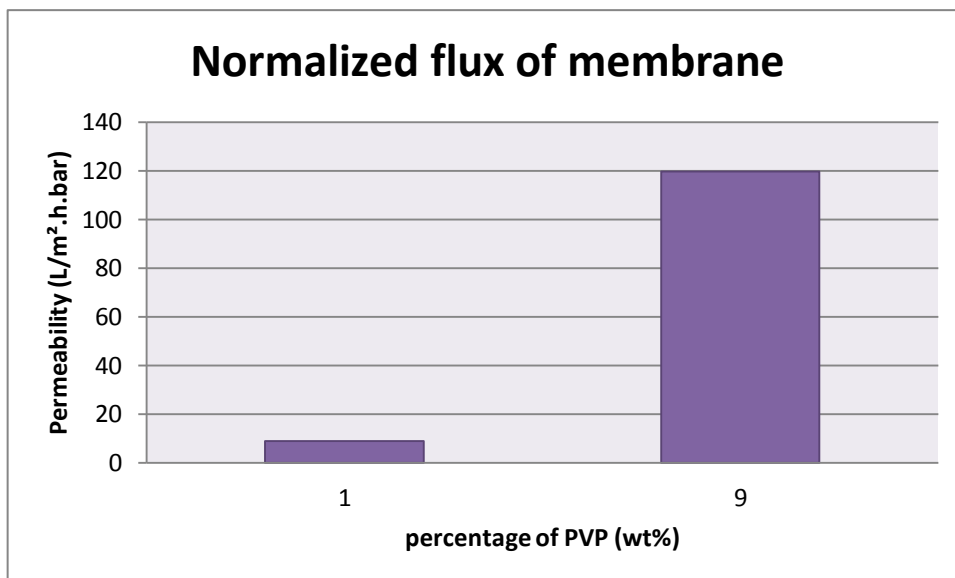


**Figure 4.2** Normalized flux for membrane A and B

### 4.3 HPLC Analysis

#### 4.3.1 Xylose and Glucose concentration

The concentration of xylose and glucose can be determined by using graphical method. As we can see from figure area obtained from the peak can determine the value at calibration curve by insert the value into the equation  $y = mx + c$  which  $y$  is area,  $m$  is slope,  $x$  is concentration and  $c$  is intercept.

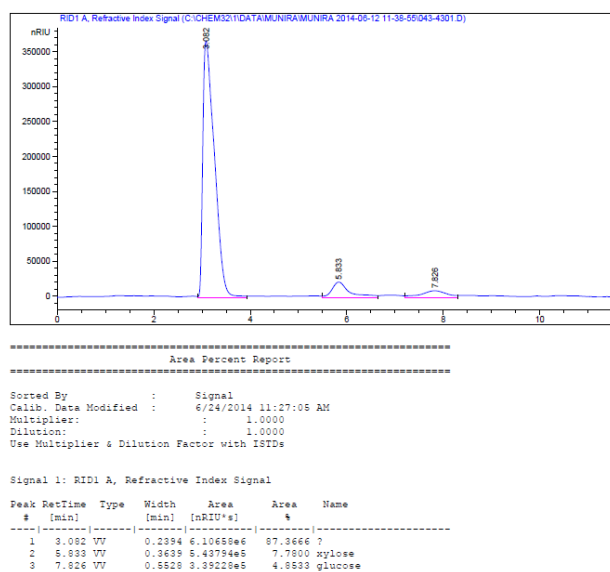
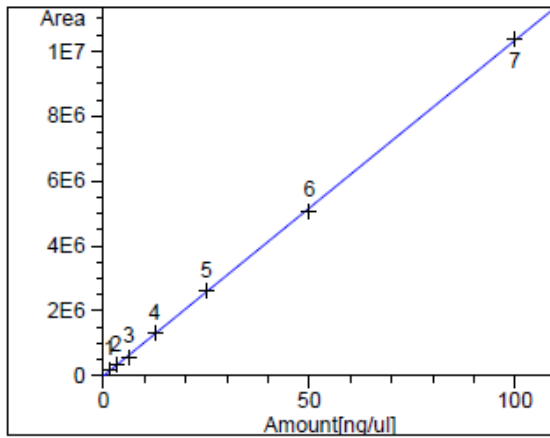
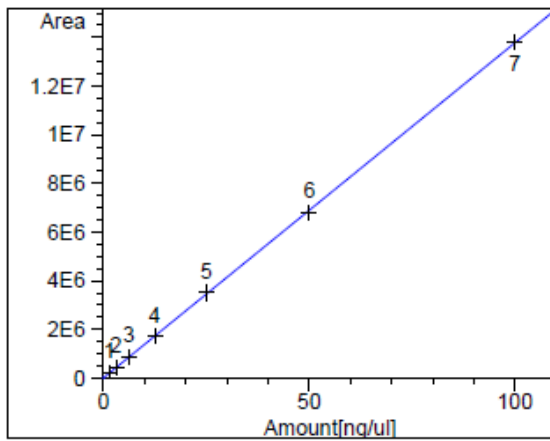


**Figure 4.3** Peak and area for xylose and glucose from HPLC analysis

=====  
Calibration Curves  
=====



xylose at exp. RT: 5.833  
RID1 A, Refractive Index Signal  
Correlation: 0.99992  
Residual Std. Dev.: 48984.69235  
Formula:  $y = mx + b$   
m: 103503.06187  
b: -7947.31229  
x: Amount  
y: Area



glucose at exp. RT: 7.943  
RID1 A, Refractive Index Signal  
Correlation: 0.99997  
Residual Std. Dev.: 39929.56478  
Formula:  $y = mx + b$   
m: 137828.79402  
b: 6645.32301  
x: Amount  
y: Area

=====  
**Figure 4.4** Calibration curve for xylose and glucose  
=====



### 4.3.2 Acetic Acid

Step to determine for acetic acid concentration was similar with step to determine xylose and glucose. The concentration of acetic acid also can be determined by using graphical method. As we can see from figure area obtained from the peak can determine the value at calibration curve by insert the value into the equation  $y = mx + c$  which y is area, m is slope, x is concentration and c is intercept.

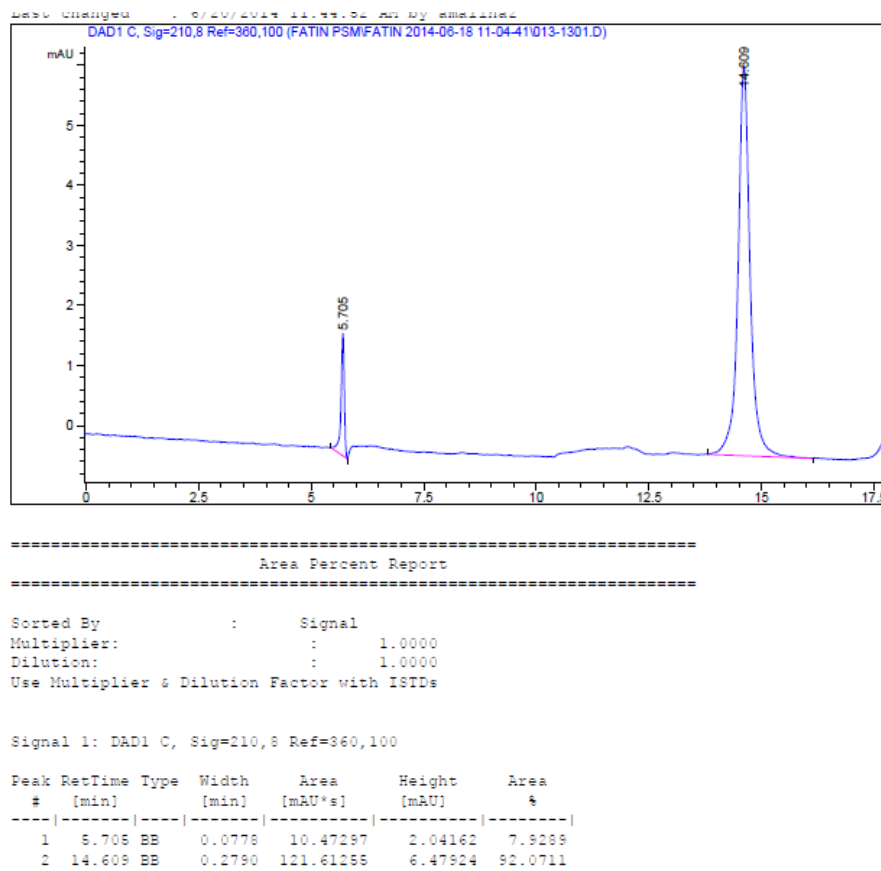
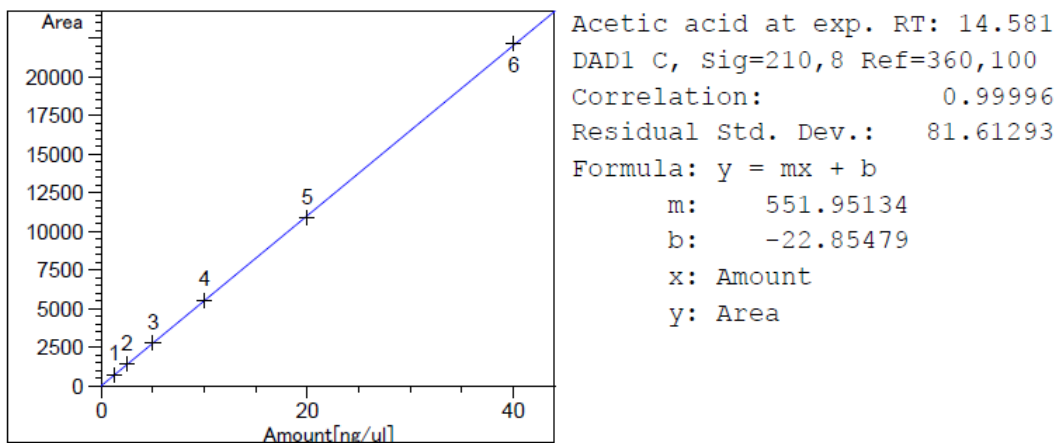


Figure 4.5 Peak and area for acetic acid from HPLC analysis

=====  
Calibration Curves  
=====



**Figure 4.6** Calibration curve for acetic acid

**Table 4.2** Concentration obtain from separation for membrane A ( 20wt% PES,1wt% PVP and 79 wt% NMP)

Type of Solution	Feed Conc.(g/L)	Feed Vol. (L)	Mass(g)	Retentate		Permeate			
				Flow Rate(m <sup>3</sup> /L)	Vol (m <sup>3</sup> )	Flowrate(ml/Min)	Vol(ml)	Conc.(g/L)	Mass (g)
glucose	3.122272144	2	10	152	1984	1.6	16	3.559234	0.056947744
xylose	6.187646917	2	10	148	1983	1.7	17	3.0905	0.0525385
acetic acid	9.944004738	2	10	140	1980	2	20	0.261739	0.00523478

**Table 4.3** Concentration obtain from separation for membrane B ( 20wt% PES,9 wt% PVP and 71 wt% NMP)

Type of Solution	Feed Conc.(g/L)	Feed Vol. (L)	Mass(g)	Retentate		Permeate			
				Flow Rate(m <sup>3</sup> /L)	Vol (m <sup>3</sup> )	Flowrate(ml/Min)	Vol(ml)	Conc.(g/L)	Mass (g)
glucose	3.122272144	2	10	152	1593	40.7	407	2.811815	1.144408705
xylose	6.187646917	2	10	148	1550	45	450	5.57168	2.507256
acetic acid	9.944004738	2	10	140	1500	50	500	9.878928	4.939464

**Table 4.4** Concentration obtain from separation for membrane A ( 20wt% PES,1wt% PVP and 79 wt% NMP) in hydrolysate solution

Type of Solution	Feed Conc.(g/L)	Feed Vol. (L)	Mass(g)	Retentate		Permeate			
				Flow Rate(m <sup>3</sup> /L)	Vol (m <sup>3</sup> )	Flowrate(ml/Min)	Vol(ml)	Conc.(g/L)	Mass (g)
glucose	3.122272144	2	6.244544	153	1983	1.5	17	0.211279	0.003591736
xylose	8.154070972	2	16.30814	149	1982	1.8	19	3.090524	0.058719961
acetic acid	1.273853851	2	2.547708	140	1978	2	22	1.231855	0.027100805

**Table 4.5** Concentration obtain from separation for membrane B ( 20wt% PES,9wt% PVP and 71 wt% NMP) in hydrolysate solution.

Type of Solution	Feed Conc.(g/L)	Feed Vol. (L)	Mass(g)	Retentate		Permeate			
				Flow Rate(m <sup>3</sup> /L)	Vol (m <sup>3</sup> )	Flowrate(ml/Min)	Vol(ml)	Conc.(g/L)	Mass (g)
glucose	3.122272144	2	6.244544	154	1594	40.6	406	2.165532	0.87920603
xylose	8.154070972	2	16.30814	148	1549	45.1	451	5.57168	2.512827609
acetic acid	1.273853851	2	2.547708	140	1523	47.7	477	2.886341	1.376784888

**Table 4.6** Flux of concentration at pressure 5 bar (L/m<sup>2</sup>.h.bar)

Membrane	xylose	glucose	Acetic Acid	Hydrolyzate		
				xylose	glucose	acetic acid
<b>A</b>	0.12882	0.12124	0.15155	0.14397	0.12882	0.16671
<b>B</b>	4.54669	4.11223	5.05188	4.55679	4.10212	4.819493

Base on the figure 4.7, it shows that increase the concentration of PVP will decrease the rejection of the component. It is because increasing the concentration of PVP will increase the number of pore at the membrane and resulting in permeability of the membrane which increase of concentration of PVP will increase the permeability of the membrane. The increasing of additive concentration tends to increase the salt permeability while reducing the effective membranes thickness. In this case, the thickness of the effective membrane layer (dense layer) is very important and well known as one of the determining factors influencing the membranes separation ability.

**Table 4.7** Rejection value of xylose, glucose and acetic acid for each concentration of PVP

Concentration (%)	solution	mass feed (g)	mass permeate (g)	Rejection (%)
1	xylose	10	0.0525385	99.474615
	glucose	10	0.056947744	99.43052256
	acetic acid	10	0.00523478	99.9476522
9	xylose	10	2.507256	74.92744
	glucose	10	2.507256	74.92744
	acetic acid	10	4.939464	50.60536

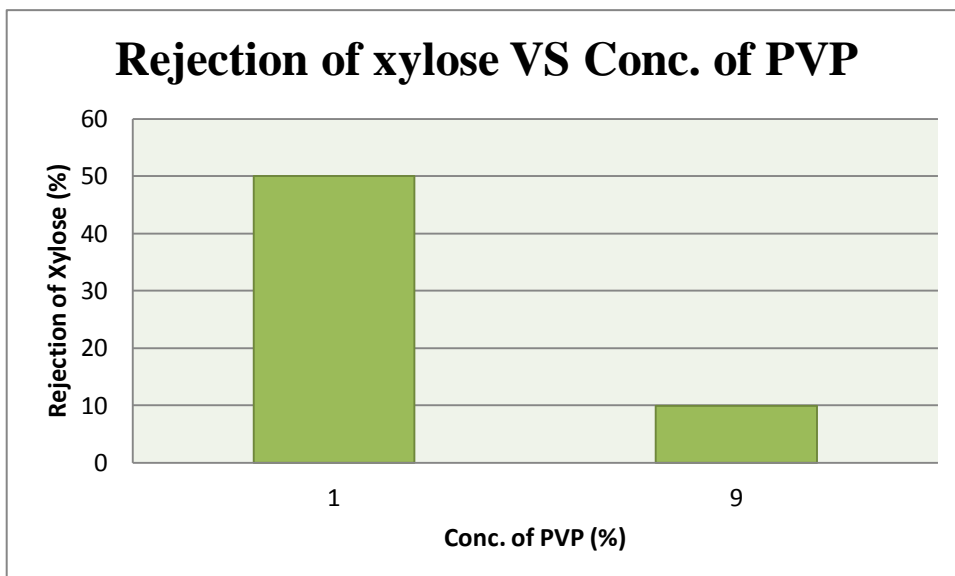


**Figure 4.7** Percentage of rejection for xylose in different concentration of NMP.

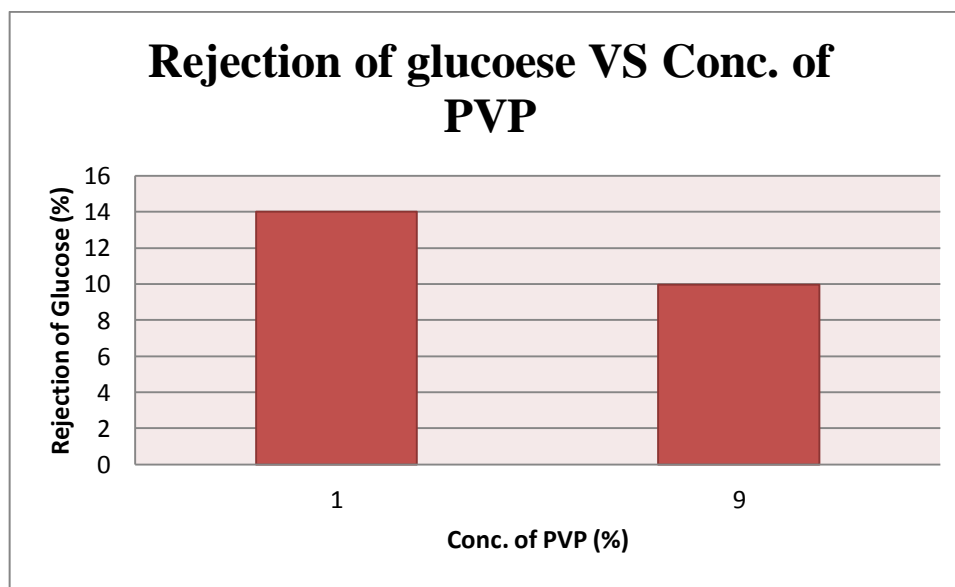


**Figure 4.8** Percentage of rejection for glucose in different concentration of NMP.

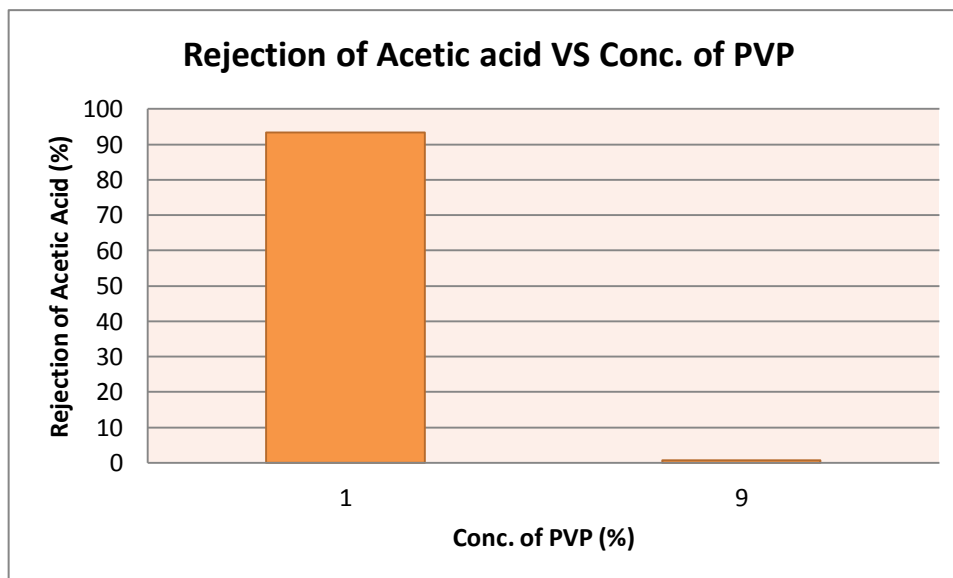


**Figure 4.9** Percentage of rejection for acetic acid in different concentration of NMP.

**Table 4.7** Rejection value of xylose, glucose and acetic acid in hydrolysate for each concentration of PVP

Concentration (%)	solution	mass feed (g)	mass permeate (g)	Rejection (%)
1	xylose	16.30814194	0.058719961	99.6399347
	glucose	6.244544287	0.003591736	99.94248201
	acetic acid	2.547707702	0.027100805	98.93626712
9	xylose	16.30814194	2.512827609	84.59157629
	glucose	6.244544287	0.87920603	85.92041325
	acetic acid	2.547707702	1.376784888	45.95985689

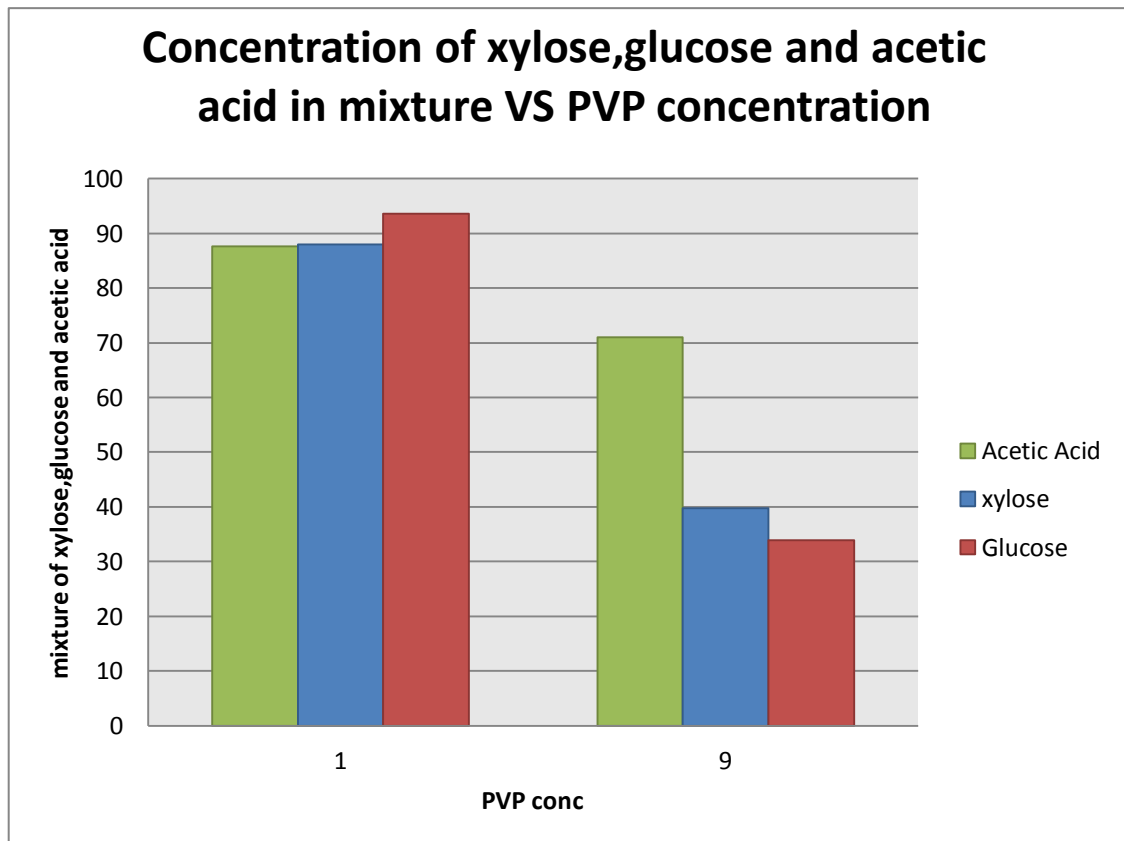


**Figure 4.10** Graph of percentage for rejection of hydrolysate in different concentration of PVP

Base on figure 4.8, it shows that 9wt % give lowest rejection compared with 1wt%. Based on the graph, we can see that acetic acid is the highest rejection compare to xylose and glucose. We can conclude that acetic acid can be remove as the retentate of the separation process.



## **5 CONCLUSION AND RECOMMENDATION**

### **5.1 Conclusion**

The combination of theoretical models and experimental data allowed the determination of membrane performance and the deduction of membranes morphological structure, thus offering a better understanding on the effect of additive concentration on the membranes performance and morphological structure of PES nanofiltration membranes separation process. Based on this study, the following conclusions have been made:

- (1) The addition of additive into polymer solutions significantly alters membrane morphological structure thus directly affecting membranes separation performance.
- (2) As additive concentration is increased, the membranes possess thinner top layer. In addition, the number of membranes pore has been increasing while the macrovoids have been disappearing. This phenomenon resulted in a higher membranes flux without compromising membranes rejection.
- (3) Acetic acid is remove from the sugar since the molecular weight of the acetic acid is smaller than both xylose and glucose.

### **5.2 Recommendation**

There are some recommendations and further study can be done on the production of nanofiltration hollow fibre membrane:

- i. Various the concentration to identify which concentration of PVP is the best
- ii. Spinning parameter should be various to determine which parameter is better to produce good separation
- iii. Change the synthetic hydrolyzate with real hydrolyzate to identify the effectiveness of the membrane

## REFERENCES

Boom R.M., Weink I.M., T. van den Boomgaard, C.A. Smolders, *Microstructures in phase inversion membranes. Part 2. The role of a polymeric additive*, J. Membr. Sci. 73 (1992) 277.

Converti A., Dominguez J.M., Perego P., Silva S.S., Zilli M. (2000), *Wood hydrolysis and hydrolyzate detoxification for subsequent xylitol production*, Chem. Eng. Technol. 23 1013–1020.

Chen W.H., Xu Y.Y, Hwang W.S., Wang J.B (2011), *Pretreatment of rice straw using an extrusion/extraction process at bench-scale for producing cellulosic ethanol*, Bioresource Technology 102, 10451–10458.

Canilha, L., Carvalho, W., Felipe, M.G.A., & Silva, J.B.A. (2008) *Xylitol production from wheat straw hemicellulosic hydrolysate: hydrolysate detoxification and carbon source used for inoculum preparation*. Brazilian J Microbiol., Vol. 39, pp. 333-336.

Chandel, A.K. & Singh, O.V. (2011) *Weedy lignocellulosic feedstock and microbial metabolic engineering: Advancing the generation of 'Biofuel'*. Appl. Microbiol. Biotechnol., Vol.89, pp. 1289-1303.

Feng, C.S., Shi, B., Li G., Wu Y. (2004), *Preparation and properties of microporous membrane from poly(vinylidene fluoride-cotetrafluoroethylene) (F2.4) for membrane distillation*, Journal of Membrane Science 237 15–24.

Feng C.Y. et al. (2013). *Recent progresses in polymeric hollow fiber membrane preparation, characterization and applications*. Separation and Purification Technology 111, 43–71

Han, M. Cheryan (1995), *Nanofiltration of model acetate solutions*, J. Membr. Sci. 107 107–113.

Hof, J.A. van't, Reuvers, A.J., Boom, R.M., Rolevink, H.H.M., Smolders, C.A. (1992), *Preparation of asymmetric gas separation membranes with high selectivity by a dual-bath coagulation method*, *J. membrane. Sci.*, 70, 17-30

Ismail A.F., Hassan A.R. (2007), *Effect of additive contents on the performances and structural properties of asymmetric polyethersulfone (PES) nanofiltration membranes*, *Separation and Purification Technology* 55 98–109

Ismail A.F. et. al (1999), *Production of super selective polysulfone hollow fiber membranes for gas separation*, *Polymer* 40 6499–6506

Jung B., Yoon J.K., Kim B., H.-W. Rhee (2004), *Effect of molecular weight of polymeric additives on formation, permeation properties and hypochlorite treatment of asymmetric polyacrylonitrile membranes*, *J. Membr. Sci.* 243 45–57.

Li, S.-G., Koops, G.H., Mulder, M.H.V., van den Boomgaard, T. and Smolders, C.A. (1994), *Wet spinning of integrally skinned hollow fiber membranes by a modified dual-bath coagulation method using a triple spinneret*. *J. Membrane Sci.*, 94, 329-340.

Lafreniere L.Y., Talbot F.D.F., Matsuura T., S. Sourirajan (1987), *Effect of polyvinylpyrrolidone additive on the performance of polyethersulfone ultrafiltration membranes*, *Ind. Eng. Chem. Res.* 26 2385.

Larsson, S., Reimann, A., Nilvebrant, N. & Jonsson, L.J. (1999a) *Comparison of different methods for the detoxification of lignocellulose hydrolysates of spruce*. *Appl. Biochem. Biotechnol.*, Vol. 77–79, pp. 91–103.

Han M.J., Nam S.T. (2002), *Thermodynamic and rheological variation in polysulfone solution by PVP and its effect in the preparation of phase inversion membranes*, *J. Membr. Sci.* 202 55

Han I.S., Cheryan M (1995)., *Nanofiltration of model acetate solutions*, *J. Membr. Sci.* 107 107–113.

Han I.S. , Cheryan M., *Downstream processing of acetate fermentation broths by nanofiltration*, Appl. Biochem. Biotechnol. 57–8 (1996) 19–28.

Marchese J., Ponche M., Ochoa N.A., Pradanos P., Palacio L., A. Hernandez (2003), *Fouling behaviour of polyethersulfone UF membranes made with different PVP*, J. Membr. Sci. 211 1.

Mulder, M. (1996). *Basic principles of membrane technology*. Amsterdam: Kluwer Academic Publishers.

Mussatto S.I., Roberto I.C. (2004), *Alternatives for detoxification of diluted-acid lignocellulosic hydrolyzates for use in fermentative processes: a review*, Bioresour. Technol. 93 1–10.

Murphy, J.D., McCarthy, K. (2005), *Ethanol production from energy crops and wastes for use as a transport fuel in Ireland*. Applied energy 82, pp. 148-166.

Murthy, G., Sridhar, S., Shyam Sunder, M., Shankaraiah, B., Ramakrishna, M., (2005). *Concentration of xylose reaction liquor by nanofiltration for the production of xylitol sugar alcohol*. Sep. Purif. Technol. 44, 221–228.

Palmqvist E., Hahn-Hägerdal B (2000)., *Fermentation of lignocellulosic hydrolyzates I: inhibition and detoxification*, Bioresour. Technol. 74 17–24.

Palmqvist E., Hahn-Hägerdal B (2000), *Fermentation of lignocellulosic hydrolyzates. II: inhibitor and mechanisms of inhibition*, Bioresour. Technol. 74 25–33.

Prakasham, R.S., Rao, R.S. & Hobbs, P.J. (2009) *Current trends in biotechnological production of xylitol and future prospects*. Curr. Trends Biotechnol. Phar., Vol. 3, pp.8-36.

Pepinster, M. ( 2007), *Analysis of ethanol production from biomass for transportation uses*. Semester project, LENI/EPFL.

Pesek SC, Koros WJ (1994). *Journal of Membrane Science*; 88:1.

Pinelo, M., Jonsson, G., Meyer, A.S., (2009). *Membrane technology for purification of enzymatically produced oligosaccharides: molecular and operational features affecting performance*. *Sep. Purif. Technol.* 70, 1–11.

Qi, B., Luo, J., Chen, X., Hang, X., Wan, Y.,(2011). *Separation of furfural from monosaccharides by nanofiltration*. *Bioresour. Technol.* 102, 7111–7118.

Qin J.J., Chung T.S. (1999), *Effect of dope flow rate on morphology, separation performance, thermal and mechanical properties of ultrafiltration hollow fiber membranes*, *J. Membr. Sci.* 157 35.

Rodrigues, R.C.L.B., Felipe, M.G.A., Almeida e Silva, J.B., Vitolo, M. & Villa, P.V. (2001) *The influence of pH, temperature and hydrolysate concentration on the removal of volatile and non-volatile compounds from sugarcane bagasse hemicellulosic hydrolysate treated with activated charcoal before or after vacuum evaporation*. *Brazilian J Chem. Engin.*, Vol. 18, pp. 299–311.

Sjöman, E., Mänttari, M., Nyström, M., Koivikko, H., Heikkilä, H., (2007). *Separation of xylose from glucose by nanofiltration from concentrated monosaccharide solutions*. *J. Membr. Sci.* 292, 106–115

Sjöman, E., Mänttari, M., Nyström, M., Koivikko, H., Heikkilä, H., 2008. *Xylose recovery by nanofiltration from different hemicellulose hydrolyzate feeds*. *J. Membr. Sci.* 310, 268–277

van den Boomgaard, A and Strathmann, H. (1998), *Membrane Formation By Phase Inversion In Multicomponent Polymer Systems, Mechanisms And Morphologies*, pg 2-3

Weng, Y.H., Wei, H.J., Tsai, T.Y., Chen, W.H., Wei, T.Y., Hwang, W.S., Wang, C.P.,Huang, C.P., (2009). *Separation of acetic acid from xylose by nanofiltration*. *Sep. Purif. Technol.* 67, 95–102.

Weng, Y.H., Wei, H.J., Tsai, T.Y., Lin, T.H., Wei, T.Y., Guo, G.L., Huang, C.P., (2010). *Separation of furans and carboxylic acids from sugars in dilute acid rice straw hydrolyzates by nanofiltration*. *Bioresour. Technol.* 101, 4889–4894.

Wilson J.J., Deschatelets L., Nishikawa N.K., *Comparative fermentability of enzymatic and acid hydrolyzates of steam-pretreated aspenwood hemicellulose by Pichia stipitis* CBS 5776, *Appl. Microbiol. Biotechnol.* 31 (1989) 592–596.

Wilson, J.J., Deschatelets, L. & Nishikawa, N.K. (1989) *Comparative fermentability of enzymatic and acid hydrolysates of steam pretreated aspen wood hemicellulose by Pichia stipitis* CBS 5776. *Appl. Microbiol. Biotechnol.*, Vol. 31, pp. 592-596.

Yu-HsiangWeng, et. al, (2009), *Separation of acetic acid from xylose by nanofiltration*, *Separation and Purification Technology* 67 95–102

## **APPENDICES**

=====  
 Calibration Table  
 =====

Calib. Data Modified : Tuesday, June 24, 2014 11:19:14 AM

Rel. Reference Window : 5.000 %  
 Abs. Reference Window : 0.000 min  
 Rel. Non-ref. Window : 5.000 %  
 Abs. Non-ref. Window : 0.000 min  
 Uncalibrated Peaks : not reported  
 Partial Calibration : Yes, identified peaks are recalibrated  
 Correct All Ret. Times: No, only for identified peaks

Curve Type : Linear  
 Origin : Included  
 Weight : Equal

Recalibration Settings:  
 Average Response : Average all calibrations  
 Average Retention Time: Floating Average New 75%

Calibration Report Options :  
 Printout of recalibrations within a sequence:  
 Calibration Table after Recalibration  
 Normal Report after Recalibration  
 If the sequence is done with bracketing:  
 Results of first cycle (ending previous bracket)

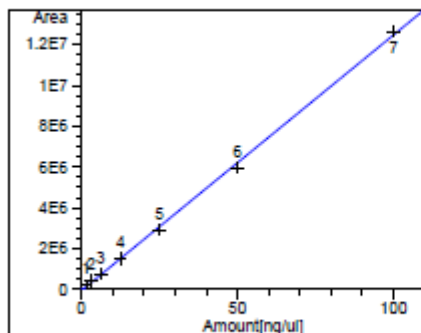
Signal 1: RID1 A, Refractive Index Signal

RetTime [min]	Lvl Sig	Amount [ng/ul]	Area	Amt/Area	Ref Grp Name
5.799	1	1.56300	2.04691e5	7.63590e-6	xylose
	2	3.12500	4.09138e5	7.63801e-6	
	3	6.25000	7.56395e5	8.26287e-6	
	4	12.50000	1.50530e6	8.30397e-6	
	5	25.00000	2.92159e6	8.55699e-6	
	6	50.00000	5.96884e6	8.37684e-6	
	7	100.00000	1.26398e7	7.91153e-6	

=====  
 Peak Sum Table  
 =====

\*\*\*No Entries in table\*\*\*  
 =====

=====  
 Calibration Curves  
 =====



xylose at exp. RT: 5.799  
 RID1 A, Refractive Index Signal  
 Correlation: 0.99954  
 Residual Std. Dev.: 142912.25148  
 Formula:  $y = mx + b$   
 m: 125467.74352  
 b: -61480.10870  
 x: Amount  
 y: Area



=====  
 Calibration Table  
 =====

Calib. Data Modified : 6/24/2014 11:15:51 AM

Rel. Reference Window : 5.000 %  
 Abs. Reference Window : 0.000 min  
 Rel. Non-ref. Window : 5.000 %  
 Abs. Non-ref. Window : 0.000 min  
 Uncalibrated Peaks : not reported  
 Partial Calibration : Yes, identified peaks are recalibrated  
 Correct All Ret. Times: No, only for identified peaks

Curve Type : Linear  
 Origin : Included  
 Weight : Equal

Recalibration Settings:  
 Average Response : Average all calibrations  
 Average Retention Time: Floating Average New 75%

Calibration Report Options :  
 Printout of recalibrations within a sequence:  
 Calibration Table after Recalibration  
 Normal Report after Recalibration  
 If the sequence is done with bracketing:  
 Results of first cycle (ending previous bracket)

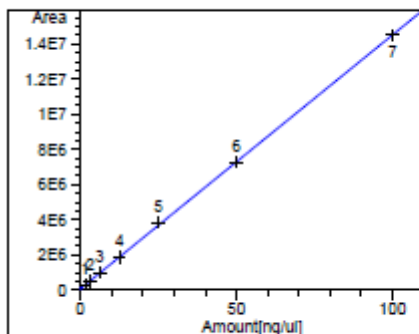
Signal 1: RID1 A, Refractive Index Signal

RetTime [min]	Lvl Sig	Amount [ng/ul]	Area	Amt/Area	Ref Grp Name
8.032	1	1.56300	2.95590e5	5.28773e-6	Glucose
	2	3.12500	5.00389e5	6.24514e-6	
	3	6.25000	9.78227e5	6.38911e-6	
	4	12.50000	1.88571e6	6.62882e-6	
	5	25.00000	3.84248e6	6.50622e-6	
	6	50.00000	7.26407e6	6.88219e-6	
	7	100.00000	1.45089e7	6.89230e-6	

=====  
 Peak Sum Table  
 =====

\*\*\*No Entries in table\*\*\*  
 =====

=====  
 Calibration Curves  
 =====



Glucose at exp. RT: 8.032  
 RID1 A, Refractive Index Signal  
 Correlation: 0.99991  
 Residual Std. Dev.: 72920.61335  
 Formula: y = mx + b  
 m: 144548.80710  
 b: 73927.72320  
 x: Amount  
 y: Area

=====  
 Calibration Table  
 =====

Calib. Data Modified : Wednesday, June 18, 2014 1:21:15 PM

Rel. Reference Window : 5.000 %  
 Abs. Reference Window : 0.000 min  
 Rel. Non-ref. Window : 5.000 %  
 Abs. Non-ref. Window : 0.000 min  
 Uncalibrated Peaks : not reported  
 Partial Calibration : Yes, identified peaks are recalibrated  
 Correct All Ret. Times: No, only for identified peaks

Curve Type : Linear  
 Origin : Included  
 Weight : Equal

Recalibration Settings:  
 Average Response : Average all calibrations  
 Average Retention Time: Floating Average New 75%

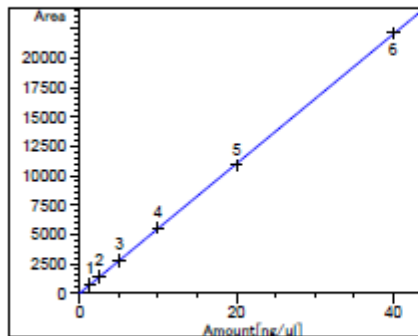
Calibration Report Options :  
 Printout of recalibrations within a sequence:  
 Calibration Table after Recalibration  
 Normal Report after Recalibration  
 If the sequence is done with bracketing:  
 Results of first cycle (ending previous bracket)

Signal 1: DAD1 C, Sig=210,8 Ref=360,100

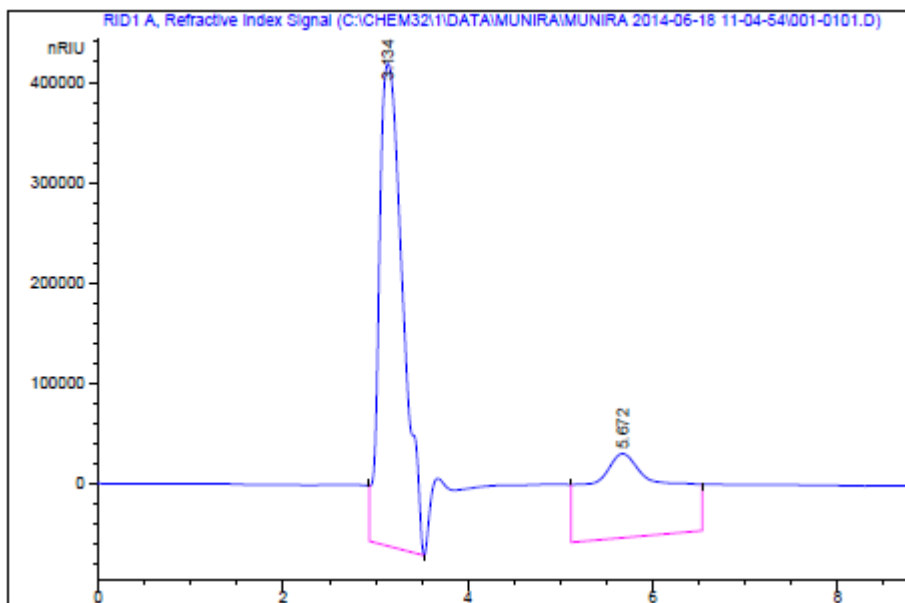
RetTime [min]	Lvl Sig	Amount [ng/ul]	Area	Amt/Area	Ref Grp Name
14.581	1 1	1.25000	690.20184	1.81107e-3	Acetic acid
	2	2.50000	1379.90149	1.81172e-3	
	3	5.00000	2736.40161	1.82722e-3	
	4	10.00000	5515.67090	1.81302e-3	
	5	20.00000	1.08551e4	1.84245e-3	
	6	40.00000	2.21289e4	1.80759e-3	

=====  
 Peak Sum Table  
 =====

=====  
 Calibration Curves  
 =====



Acetic acid at exp. RT: 14.581  
 DAD1 C, Sig=210,8 Ref=360,100  
 Correlation: 0.99996  
 Residual Std. Dev.: 81.61293  
 Formula:  $y = mx + b$   
 m: 551.95134  
 b: -22.85479  
 x: Amount  
 y: Area



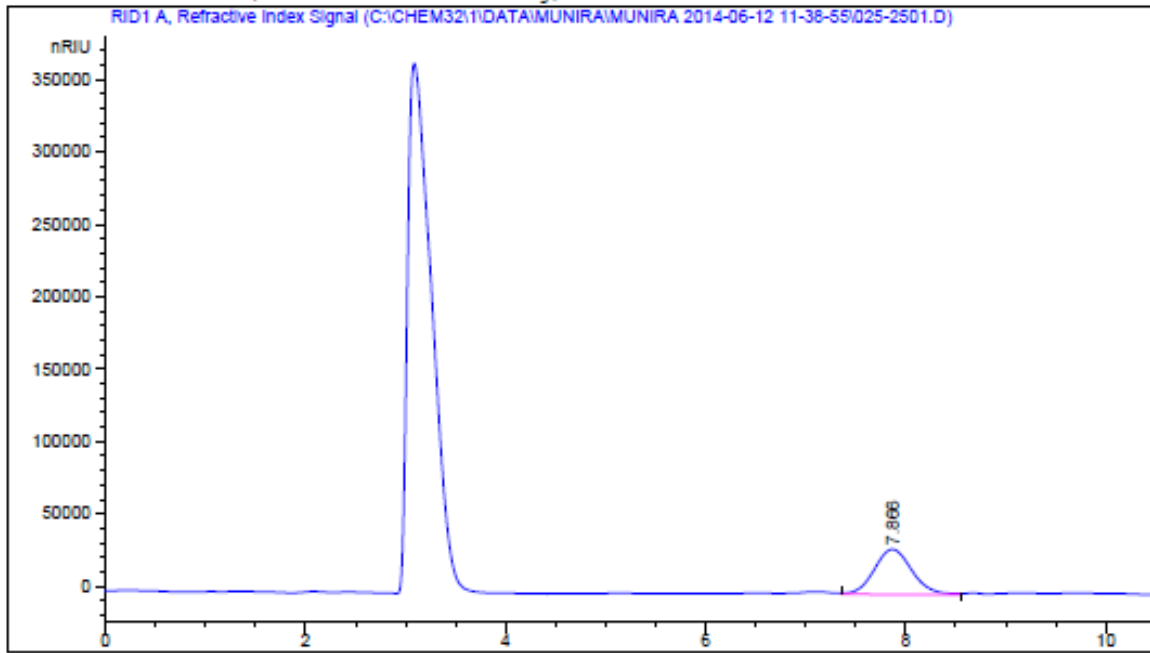
=====  
 Area Percent Report  
 =====

Sorted By : Signal  
 Calib. Data Modified : 6/24/2014 11:27:05 AM  
 Multiplier: : 1.0000  
 Dilution: : 1.0000  
 Use Multiplier & Dilution Factor with ISTDs

Signal 1: RID1 A, Refractive Index Signal

Peak #	RetTime [min]	Type	Width [min]	Area [nRIU*s]	Area %	Name
1	3.134	VV	0.2712	8.49405e6	62.6265	?
2	5.672	VV	0.7867	5.06898e6	37.3735	?
3	5.833		0.0000	0.00000	0.0000	xylose
4	7.943		0.0000	0.00000	0.0000	glucose

Totals : 1.35630e7

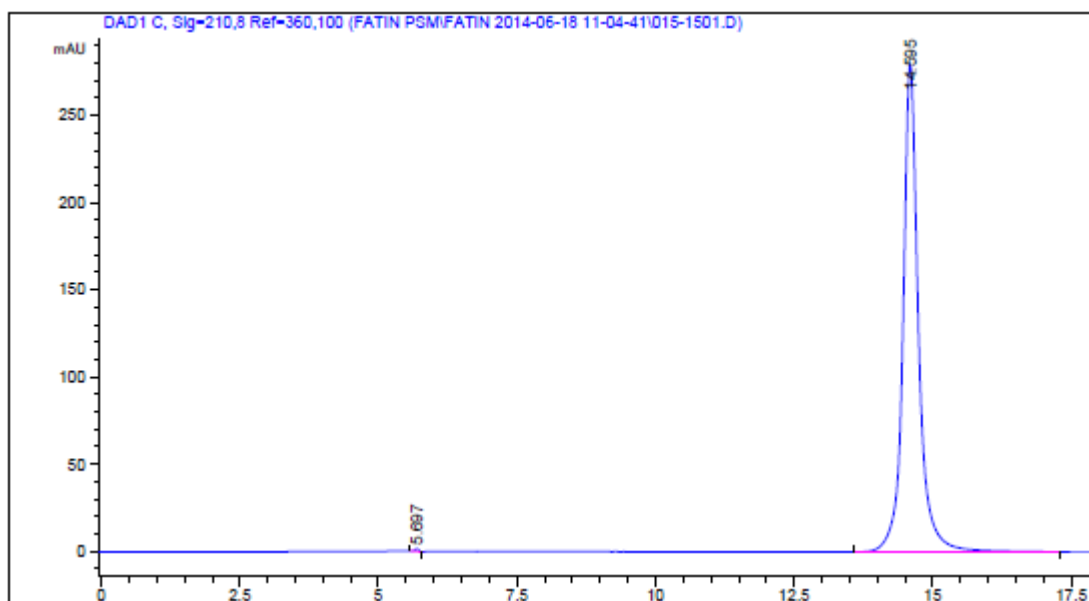


=====  
 Area Percent Report  
 =====

Sorted By : Signal  
 Calib. Data Modified : 6/24/2014 11:27:05 AM  
 Multiplier: : 1.0000  
 Dilution: : 1.0000  
 Use Multiplier & Dilution Factor with ISTDs

Signal 1: RID1 A, Refractive Index Signal

Peak #	RetTime [min]	Type	Width [min]	Area [nRIU*s]	Area %	Name
1	5.833		0.0000	0.00000	0.0000	xylose
2	7.866	VV	0.4054	8.18074e5	100.0000	glucose
Totals :				8.18074e5		



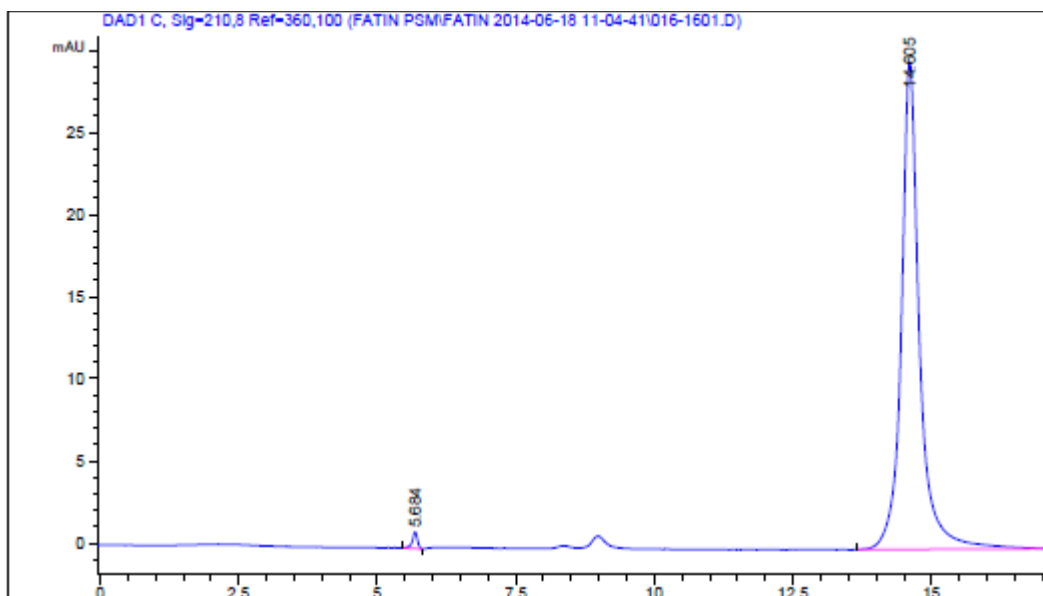
=====  
 Area Percent Report  
 =====

Sorted By : Signal  
 Multiplier: : 1.0000  
 Dilution: : 1.0000  
 Use Multiplier & Dilution Factor with ISTDs

Signal 1: DAD1 C, Sig=210,8 Ref=360,100

Peak #	RetTime [min]	Type	Width [min]	Area [mAU*s]	Height [mAU]	Area %
1	5.697	BB	0.0734	7.32040	1.54096	0.1338
2	14.898	BB	0.2879	8465.78198	279.78616	99.8662

Totals : 8473.07236 281.32712

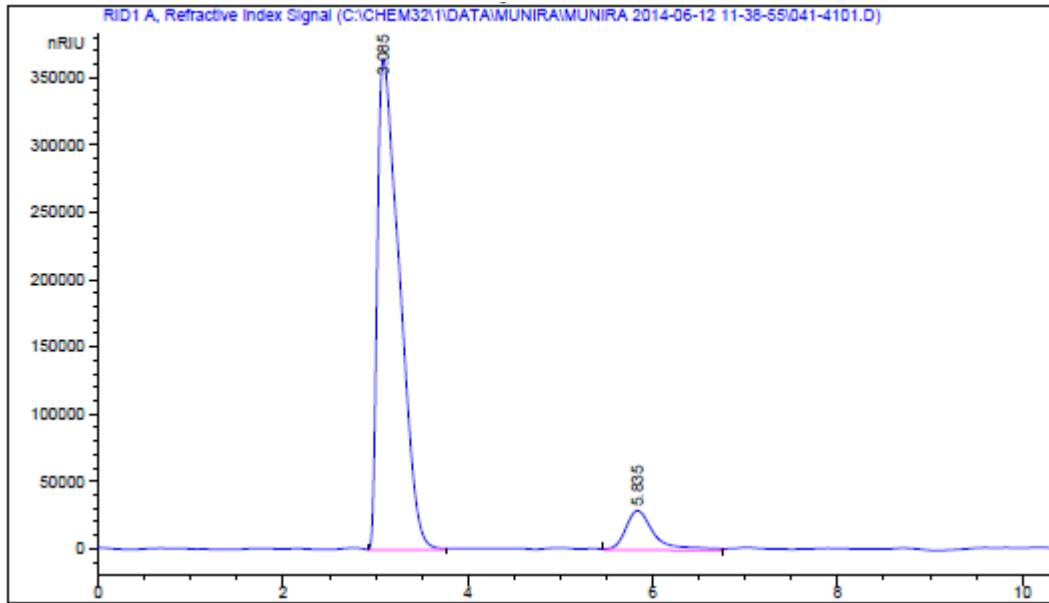


=====  
 Area Percent Report  
 =====

Sorted By : Signal  
 Multiplier: : 1.0000  
 Dilution: : 1.0000  
 Use Multiplier & Dilution Factor with ISTDs

Signal 1: DAD1 C, Sig=210,8 Ref=360,100

Peak #	RetTime [min]	Type	Width [min]	Area [mAU*s]	Height [mAU]	Area %
1	5.684	BB	0.0943	6.49414	1.02019	0.9456
2	14.605	BB	0.3214	680.25055	29.67693	99.0544

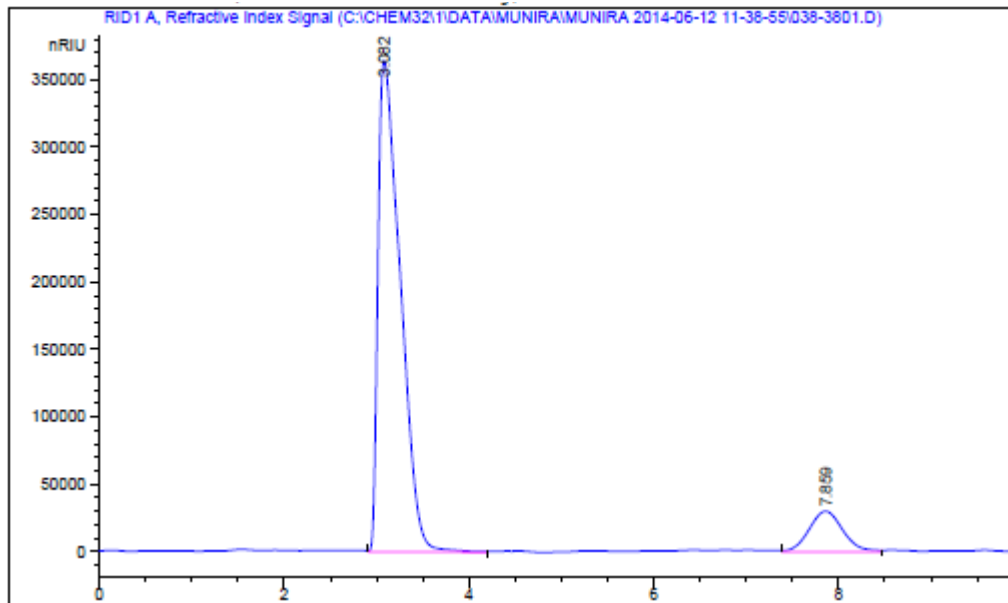


=====  
 Area Percent Report  
 =====

Sorted By : Signal  
 Calib. Data Modified : 6/24/2014 11:27:05 AM  
 Multiplier: : 1.0000  
 Dilution: : 1.0000  
 Use Multiplier & Dilution Factor with ISTDs

Signal 1: RID1 A, Refractive Index Signal

Peak #	RetTime [min]	Type	Width [min]	Area [nRIU*s]	Area %	Name
1	3.085	VV	0.2385	6.04268e6	90.4557	?
2	5.835	VV	0.3251	6.37586e5	9.5443	xylose
3	7.943		0.0000	0.00000	0.0000	glucose



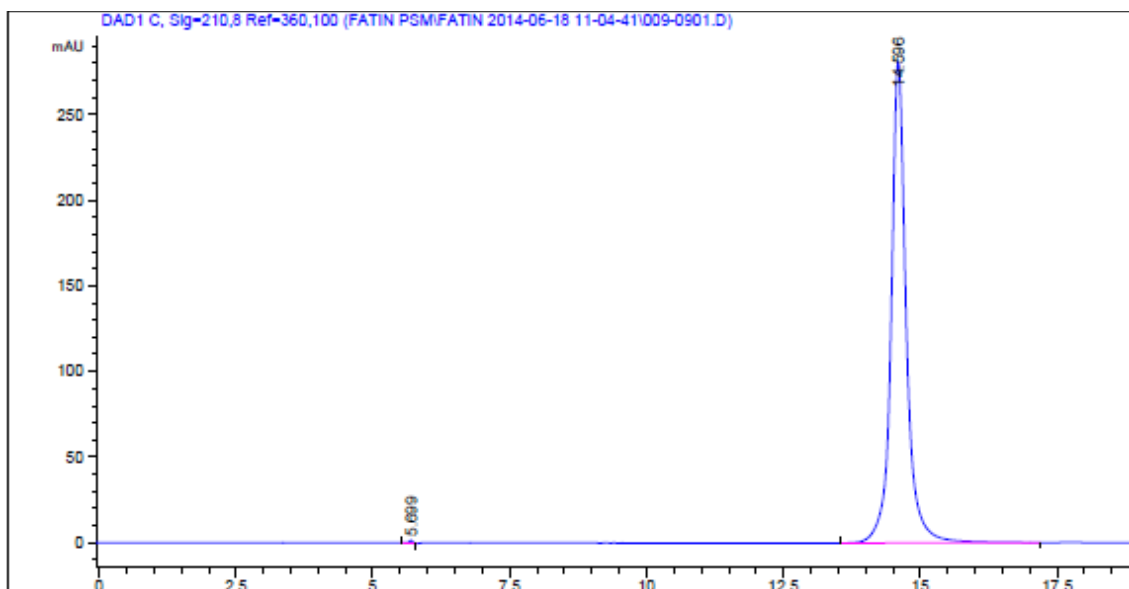
=====  
 Area Percent Report  
 =====

Sorted By : Signal  
 Calib. Data Modified : 6/24/2014 11:27:05 AM  
 Multiplier: : 1.0000  
 Dilution: : 1.0000  
 Use Multiplier & Dilution Factor with ISTDs

Signal 1: RID1 A, Refractive Index Signal

Peak #	RetTime [min]	Type	Width [min]	Area [nRIU*s]	Area %	Name
1	3.082	VV	0.2428	6.09806e6	88.6725	?
2	5.833		0.0000	0.00000	0.0000	xylose
3	7.859	VV	0.3975	7.78995e5	11.3275	glucose
Totals :				6.87705e6		





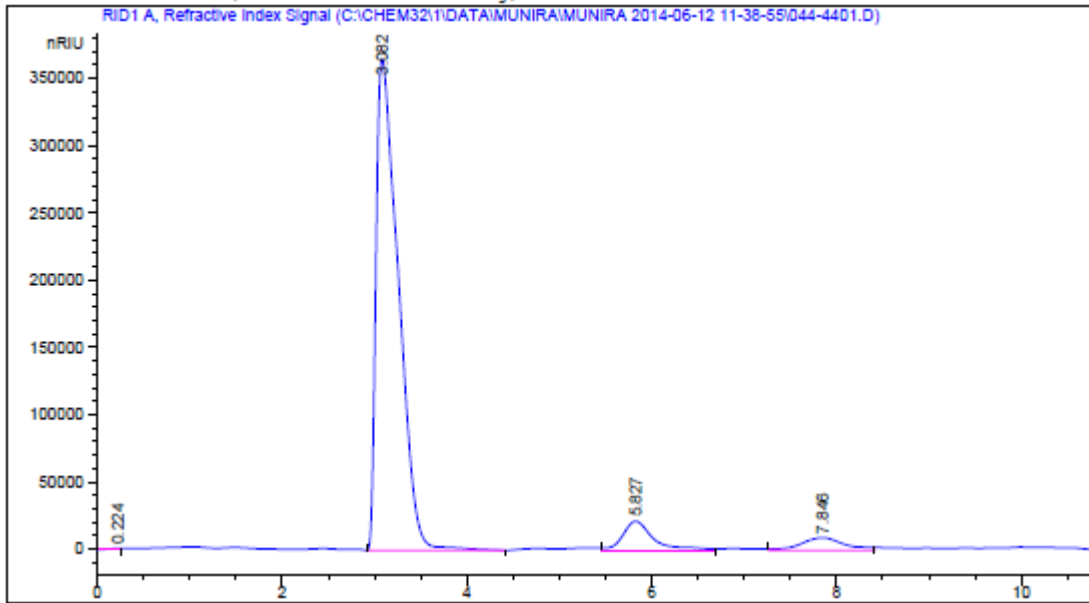
=====  
 Area Percent Report  
 =====

Sorted By : Signal  
 Multiplier: : 1.0000  
 Dilution: : 1.0000  
 Use Multiplier & Dilution Factor with ISTDs

Signal 1: DAD1 C, Sig=210,8 Ref=360,100

Peak #	RetTime [min]	Type	Width [min]	Area [mAU*s]	Height [mAU]	Area %
1	5.699	BB	0.0792	3.64844	1.64769	0.1590
2	14.896	BB	0.2852	5429.83301	281.92446	99.8410

Totals :                    5438.47845   282.97216



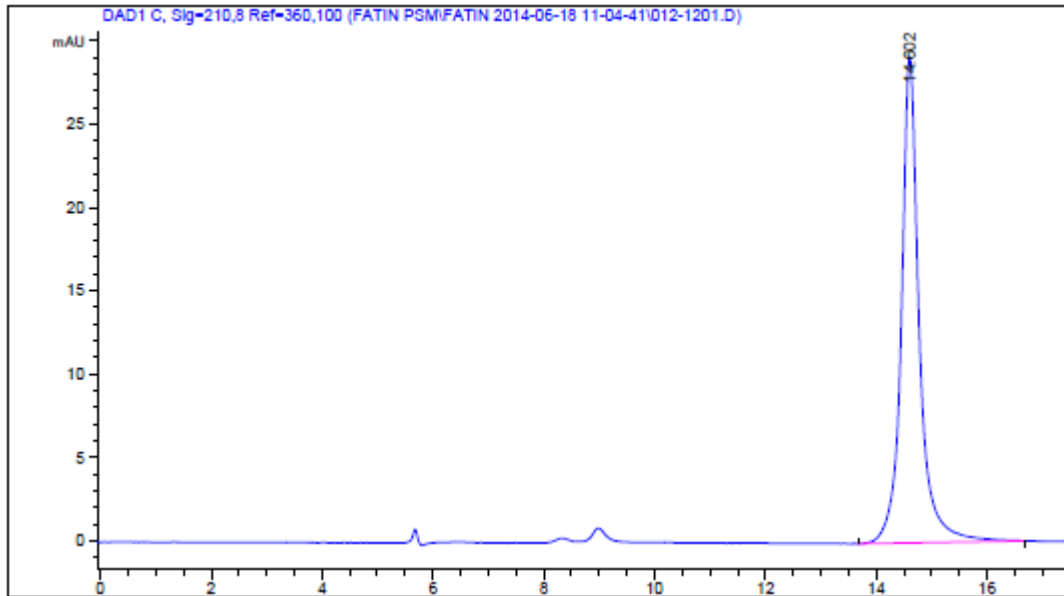
=====  
 Area Percent Report  
 =====

Sorted By : Signal  
 Calib. Data Modified : 6/24/2014 11:27:05 AM  
 Multiplier: : 1.0000  
 Dilution: : 1.0000  
 Use Multiplier & Dilution Factor with ISTDs

Signal 1: RID1 A, Refractive Index Signal

Peak #	RetTime [min]	Type	Width [min]	Area [nRIU*s]	Area %	Name
1	0.224	BV	0.1576	7435.14551	0.1076	?
2	3.082	VV	0.2399	6.09383e6	88.2278	?
3	5.827	VV	0.3390	5.00546e5	7.2470	xylose
4	7.846	VV	0.4895	3.05118e5	4.4176	glucose

Totals : 6.90693e6



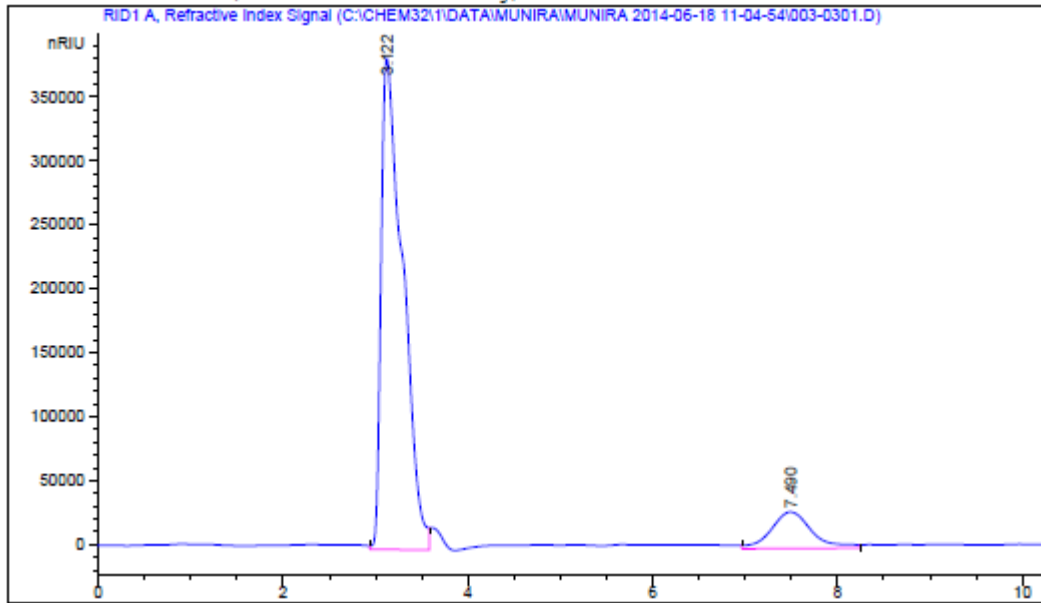
=====  
 Area Percent Report  
 =====

Sorted By : Signal  
 Multiplier: : 1.0000  
 Dilution: : 1.0000  
 Use Multiplier & Dilution Factor with ISTDs

Signal 1: DAD1 C, Sig=210,8 Ref=360,100

Peak #	RetTime [min]	Type	Width [min]	Area [mAU*s]	Height [mAU]	Area %
1	14.602	BB	0.3271	657.06909	29.13356	100.0000

Totals :                    657.06909    29.13356



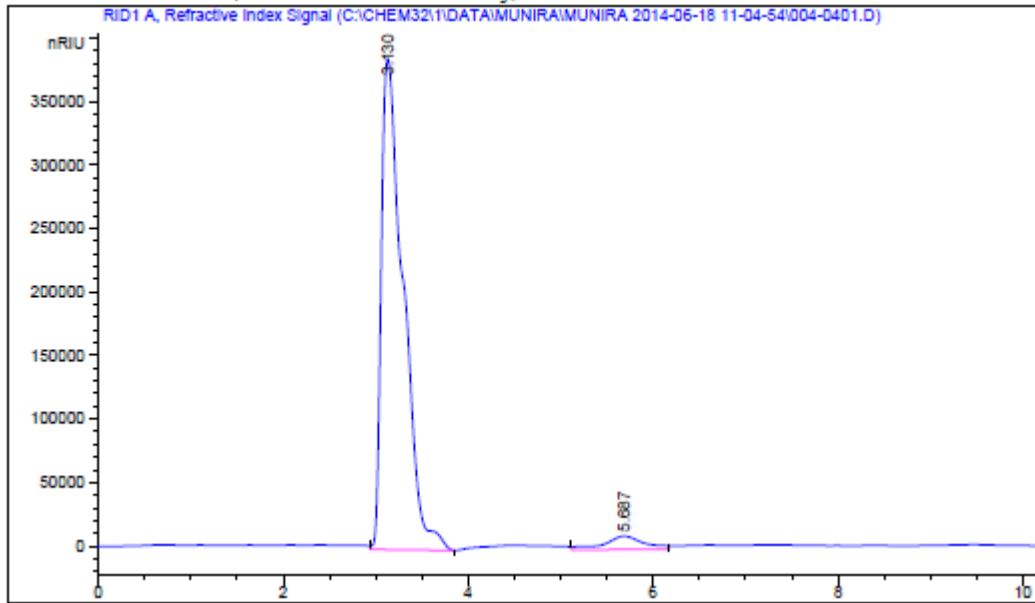
=====  
 Area Percent Report  
 =====

Sorted By : Signal  
 Calib. Data Modified : 6/24/2014 11:27:05 AM  
 Multiplier: : 1.0000  
 Dilution: : 1.0000  
 Use Multiplier & Dilution Factor with ISTDs

Signal 1: RID1 A, Refractive Index Signal

Peak #	RetTime [min]	Type	Width [min]	Area [nRIU*s]	Area %	Name
1	3.122	VV	0.2309	6.24857e6	87.7405	?
2	5.833		0.0000	0.00000	0.0000	xylose
3	7.490	VV	0.4658	8.73077e5	12.2595	?
4	7.943		0.0000	0.00000	0.0000	glucose

Totals : 7.12165e6



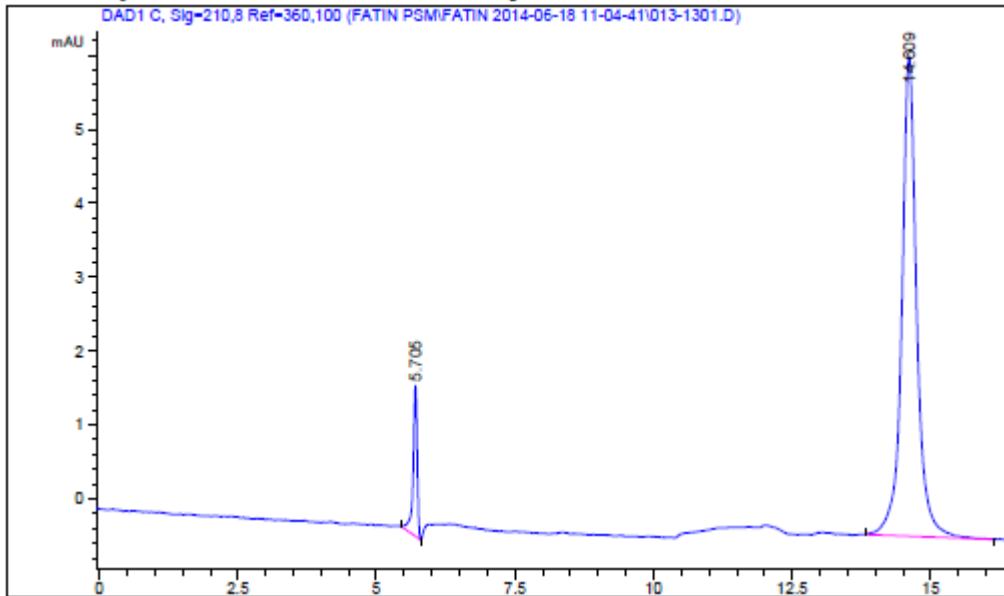
=====  
 Area Percent Report  
 =====

Sorted By : Signal  
 Calib. Data Modified : 6/24/2014 11:27:05 AM  
 Multiplier: : 1.0000  
 Dilution: : 1.0000  
 Use Multiplier & Dilution Factor with ISTDs

Signal 1: RID1 A, Refractive Index Signal

Peak #	RetTime [min]	Type	Width [min]	Area [nRIU*s]	Area %	Name
1	3.130	VV	0.2395	6.36652e6	95.1249	?
2	5.687	VV	0.4249	3.26281e5	4.8751	?
3	5.833		0.0000	0.00000	0.0000	xylose
4	7.943		0.0000	0.00000	0.0000	glucose

Totals : 6.69280e6



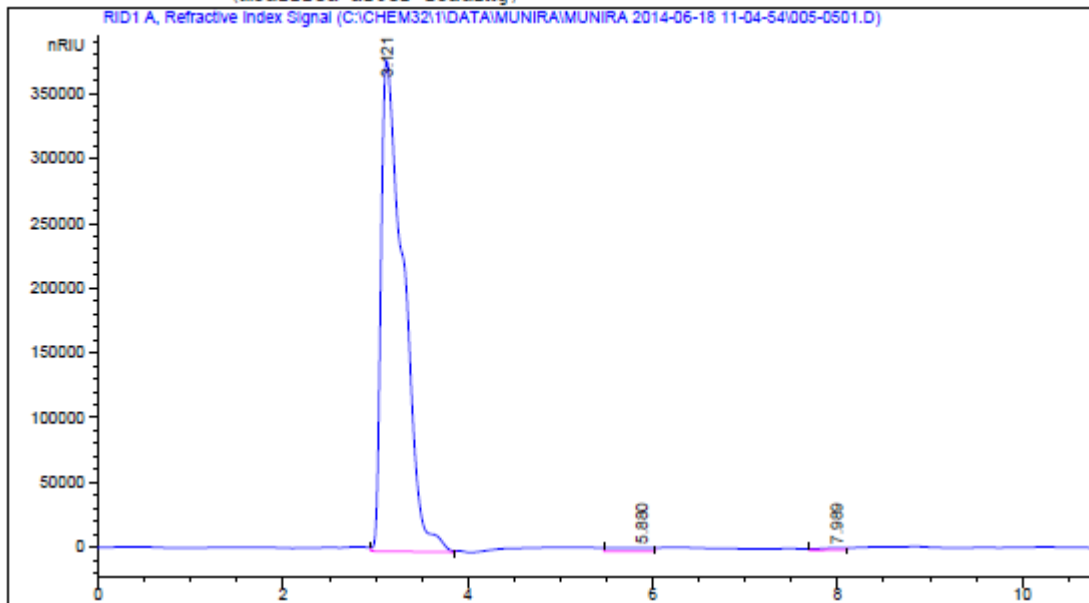
=====  
 Area Percent Report  
 =====

Sorted By : Signal  
 Multiplier: : 1.0000  
 Dilution: : 1.0000  
 Use Multiplier & Dilution Factor with ISTDs

Signal 1: DAD1 C, Sig=210,8 Ref=360,100

Peak #	RetTime [min]	Type	Width [min]	Area [mAU*s]	Height [mAU]	Area %
1	5.705	BB	0.0778	10.47297	2.04162	7.9289
2	14.609	BB	0.2790	121.61265	6.47924	92.0711

Totals : 132.08561 8.52086

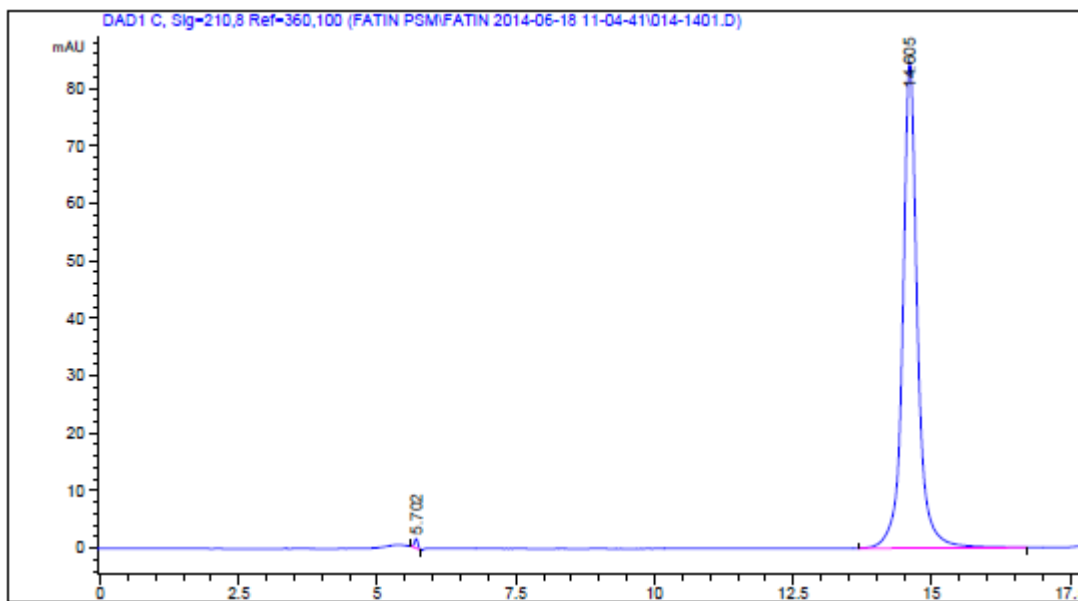


=====  
 Area Percent Report  
 =====

Sorted By : Signal  
 Calib. Data Modified : 6/24/2014 11:27:05 AM  
 Multiplier: : 1.0000  
 Dilution: : 1.0000  
 Use Multiplier & Dilution Factor with ISTDs

Signal 1: RID1 A, Refractive Index Signal

Peak #	RetTime [min]	Type	Width [min]	Area [nRIU*s]	Area %	Name
1	3.121	VV	0.2371	6.37104e6	98.0162	?
2	5.880	VV	0.4144	9.31785e4	1.4335	xylose
3	7.989	VV	0.2743	3.57656e4	0.5502	glucose
Totals :				6.49998e6		



=====  
 Area Percent Report  
 =====

Sorted By : Signal  
 Multiplier: : 1.0000  
 Dilution: : 1.0000  
 Use Multiplier & Dilution Factor with ISTDs

Signal 1: DAD1 C, Sig=210,8 Ref=360,100

Peak #	RetTime [min]	Type	Width [min]	Area [mAU*s]	Height [mAU]	Area %
1	5.702	BB	0.0669	7.27768	1.66738	0.4613
2	14.605	BB	0.2746	1870.26826	84.61730	99.5387
Totals :				1877.54294	86.28469	